Why the fermion dynamical symmetry model fails to predict nuclear masses: A comprehensive assessment

Ragnar Bengtsson
Department of Mathematical Physics, Lund Institute of Technology, P.O. Box 118, Sweden

Peter Möller
Theoretical Division, Los Alamos National Laboratory, Los Alamos, New Mexico 87545
(Received 1 March 2000; revised manuscript received 7 February 2001; published 7 June 2001)

In the last several years new experimental data have become available on alpha-decay chains starting in the predicted deformed superheavy region near $^{272}110$. This has promoted new interest in nuclear mass formulas and how well they extrapolate to regions far beyond where experimental masses were previously known. We here focus on two such mass models, namely the fermion dynamical symmetry model and the finite-range droplet model. We have chosen these models since they both reproduce previously known actinide masses with good accuracy, but rapidly diverge from each other in the region of the recently observed new elements. Furthermore, the two models have been the subject of animated discussions concerning which one gives the most reliable predictions of nuclear masses in the superheavy region and in the terminating region of the *r* process. The new data support the predictions of the finite-range droplet model. We discuss the fermion dynamical symmetry model and its application [Han *et al.*, Phys. Rev. C **45**, 1127 (1992)] to the calculation of trans-Pb nuclear masses. As will be shown, the model contains unphysical features and has many more free constants than claimed. The values obtained for the constants and the model agreement with data in the region of adjustment are therefore of no particular significance and severe divergences occur for recently discovered nuclei outside the region of adjustment.

DOI: 10.1103/PhysRevC.64.014308 PACS number(s): 21.60.Fw, 21.10.Dr

I. INTRODUCTION

In microscopic nuclear-structure calculations one cannot solve the full many-body problem with the true nucleon-nucleon force. Instead, the problem is always considerably reduced to some type of *model* with *effective* forces. Although both the model and the force used are always drastic simplifications of reality, the aim in constructing these models is that they both be solvable and retain the ability to describe and predict, at a useful level of accuracy, some set of nuclear-structure properties. We here discuss two implementations of microscopic nuclear-structure models, in particular as applied to the calculation of nuclear masses. One model is the FDSM (fermion dynamical-symmetry model) [1,2], the other the FRDM (finite-range droplet model) [3–5] version of the macroscopic-microscopic method as implemented in a series of mass calculations.

In the early 1990s the constants of both models were determined, partly from least-squares adjustments to nuclear masses. For the FDSM model, which was adjusted to Pb and trans-Pb masses only, the rms error obtained was 0.22 MeV for this restricted region. For the FRDM, which was adjusted to all known masses with proton number $Z \geqslant 8$, and neutron number $N \geqslant 8$, the model error was 0.669 MeV for this entire region of nuclei. However, the two models predicted quite different masses for unknown nuclei already a few nuclei away from the known region. For nuclei further away, notably in the superheavy region and along the upper part of the *r*-process path, the predictions of the two models diverge even more.

In the first half of the 1990s it was often debated which one of the models is the most reliable for predicting unknown masses and in a 1996 paper [6], the proponents for the FDSM model stated

The picture presented here (i.e., the FDSM model) suggests trends for the heaviest nuclei that are rather different relative to those expected in traditional mass models (one of which is FRDM). These could be tested by further observations of isotopes in the $Z=110$–114 region, by a continued failure to find superheavy elements at their historically expected location, and by observables associated with r-process element production.

Today, some years later, several new elements and isotopes in the $Z=110$–112 region have been observed. Thus some of the necessary experimental observations, needed to perform the test asked for in the 1996 FDSM paper, are now available. The test is carried out in this paper. Since the FRLDM and FDSM give very different masses in the new region, at least one of the models will have to fail this test, and we present here a detailed analysis of the reasons for this failure.

It could be argued that a model which fails does not deserve a detailed study. We are, however, of a different opinion. The approaches used in the development of the FRDM and FDSM models are very different in the strategies used to reproduce known data, in the way in which the models are simplified, in the way in which model constants are allowed to be adjusted, and finally in the approach to establish the predictive power of the models. It is therefore well justified to tell the story of these models. A detailed comparison between the FRDM and FDSM will illuminate all the points mentioned above. We are convinced that such an analysis will provide essential insights for the future.

Since an important feature of this paper is to discuss model constants and how to determine their values, including how to adjust some model constants to data by use of the method of least squares, a detailed, complete description of both models is required. To follow many of the arguments presented in this paper, such a detailed knowledge of the role of each constant and the place at which it appears in the equations is necessary. For the FRDM we are able to refer to earlier work [5,7] for such a description and complete account and counting of the constants; for the FDSM we need to perform a similar accounting of the model constants and their significance here.

We mentioned that nuclear-structure calculations are performed with *models* and *effective* forces that are severe approximations of reality but that retain ''essential features'' of the real physical system. How can one know if models such as the FDSM or the macroscopic-microscopic method as implemented in the FRDM retain essential features? There are several approaches that should be pursued in parallel. The models must be used in a large number of calculations in a consistent manner to test the models and to give experience with the models. One should use general, model-independent arguments to analyze and judge the models. For example, are the constants few enough and of a type that can be reliably determined from available data points? Do the models correctly predict new data that become available? And, the model features should be critically studied and challenged by the scientific community. It is from the interplay of such activities that useful models will evolve. It is in this spirit we offer our criticism of the FDSM and the mass formulas derived from it. The latter appear in two versions [1,2,6] of which we are mainly going to discuss version II presented in Refs. [1,6], which the authors of the FDSM papers claim to be the superior one through statements like

''*. . . version II is able to produce an excellent fit of 332 nuclei with a better rms error of 0.22 MeV (vs the 0.34 MeV of version I) and parameters that are fewer in number . . . .*''

''*Thus we have reduced the number of adjustable parameters in the FDSM-Strutinsky mass formula from 16 in version I to 13 in version II.*''

Here we comment on the above statements and on some other aspects of the FDSM model. Specifically, our discussion will address the following points:

(1) We show that the number of adjustable constants is grossly misrepresented; it is much larger than 13.

(2) The Strutinsky-like shell-correction method used in the FDSM work is unphysical. It is still plagued by many of the same deficiencies as occur when the nuclear energy is calculated as a sum of single-particle energies; deficiencies that Strutinsky removed with *his* method [8,9].

(3) It is rather trivial to achieve an error of about 0.22 MeV in a fit of a multiparameter expression to a limited region such as the ''actinide'' region the authors consider. Such results are therefore of no physical significance, they are simply a parametrization of the data.

(4) Since octupole interactions are not considered in the FDSM model one would expect larger errors in the FDSM masses where octupole deformations are important. Such errors do not occur. This observation demonstrates that the results of the FDSM model lack important physical features.

To be able to elaborate on the above points we have to outline those features of the FDSM that are necessary for our discussion. However, we shall start with a brief discussion of the macroscopic-microscopic method used in the FRDM and its application to nuclear mass calculations.

II. THE MACROSCOPIC-MICROSCOPIC METHOD

Shortly after the advent of the deformed single-particle models in the mid 1950s [10], the energy of a nucleus as a function of deformation was often calculated as a sum of three contributions: a sum of the energies of occupied single-particle levels, a Coulomb energy, and a pairing energy [11–13]. The shape of the nucleus in its ground-state configuration was obtained by minimizing the energy with respect to deformation.

Although the above method was used for calculating the nuclear potential energy versus deformation in the vicinity of the ground state, it was observed at the time that it was in principle incorrect to relate the total energy of the nucleus to the sum of single-particle level energies. However, the approach was used because it worked in practice.

After the initial successful applications of the above method to calculations of the potential energy in the vicinity of the ground state, attempts were made to apply the procedure to distortions somewhat beyond the ground state. However, here the method failed catastrophically.

At this time, no global nuclear mass calculations based on microscopic models had been made. However, global mass calculations based on liquid-drop models were carried out, for example, by Ref. [14]. In these calculations the mass was obtained as a sum of a macroscopic term plus a microscopic correction obtained from a postulated, parameterized expression. It was not known if single-particle models could at all be utilized to obtain the microscopic corrections.

A. The conventional Strutinsky shell-correction method

It was Strutinsky [8,9] who simultaneously resolved the difficulties that were associated with using sums of single-particle level energies and proposed a method for obtaining microscopic shell and pairing corrections from calculated single-particle energies of both spherical and deformed nuclei. Strutinsky observed that the sum of single-particle level energies is often very large, in heavy nuclei much more than 1000 MeV in a Nilsson modified-oscillator model, but that the change with deformation in this sum is often only a few MeV, that is, a few parts in 1000. Since the energy of the nucleus is certainly not correctly given to such an accuracy by the sum of single-particle level energies another method had to be found. Strutinsky observed that the stability of the nucleus was clearly correlated with the magnitude of the gaps in the single-particle levels, or more precisely to the level density, close to the Fermi surface. He therefore proposed that one use a macroscopic-microscopic method to calculate the nuclear potential energy of deformation in which the microscopic correction is obtained as a sum of calculated single-particle level energies minus the energy

from a smoothed-out level spectrum occupied with the same number of particles. The crucial point in Strutinsky's method is that *the smoothed-out level spectrum is obtained from the calculated single-particle levels themselves*.

Thus the smooth level density is generated from the sharp, delta-function single-particle level density by folding with a Gaussian so that the new level density is a sum of Gaussians, each of which is centered around an original level. Because the large systematic errors that are present in the sum of the single-particle level energies will also be present in the Gaussian level spectrum they will be subtracted out when the microscopic correction is calculated as the difference between these two terms.

B. Implementations of the macroscopic-microscopic method

In a macroscopic-microscopic model the nuclear energy, which is calculated as a function of shape, proton number Z, and neutron number N, is the sum of a macroscopic term and a microscopic term. Thus the total nuclear potential energy can be written as

$$E_{\rm pot}(Z,N,\text{shape}) = E_{\rm macr}(Z,N,\text{shape}) + E_{\rm micr}(Z,N,\text{shape}), \tag{1}$$

where the microscopic term in addition to the Strutinsky shell-correction energy also contains a pairing-energy contribution.

After Strutinsky had proposed his method, several groups applied it to a large number of nuclear-structure problems. The calculations could differ in the choice of macroscopic liquid-drop, microscopic single-particle, and microscopic pairing models. Several choices exist for all of these models. However, common aspects of these calculations are that a large number of nuclear-structure properties are described with relatively few constants from systems as light as ^{16}O to the heaviest elements.

The first step in a macroscopic-microscopic calculation is to select a nuclear shape of interest. Next, the macroscopic energy is calculated for this shape, and the levels in a single-particle potential with the same shape are determined. Then, the microscopic shell and pairing corrections are calculated by use of Strutinsky's method and the potential energy is obtained as the sum of the macroscopic term and the shell-plus-pairing corrections. Finally, the ground-state mass is determined by minimizing the potential energy with respect to deformation, that is the calculation is carried out for a grid of deformation points and the minimum energy on this grid is determined.

Apart from the ground-state mass a large number of nuclear-structure quantities may be determined without the introduction of any additional constants. Examples of such quantities are the quadrupole moment and higher moments of the ground-state shape, the fission-barrier saddle points and secondary minima, the energy of shape-isomeric states, and band-head energies.

C. The FRDM model

The macroscopic-microscopic FRDM (1992) model is the latest version of the ''Möller-Nix mass model'' [5]. It is completely defined in Ref. [5], where a well-defined enumeration of all the constants of the model is also made. We therefore refer to that publication for a complete discussion of the model. However, in the FDSM (1992) paper [1] frequent references are made to the FRDM in its 1988 version. To be able to comment on the discussion in Ref. [1] we enumerate in the next section the constants in the FRDM in its 1988 form, which in terms of model constants and other aspects differs only slightly from the FRDM (1992).

D. Constants of the FRDM model

It is always of interest to have a clear picture of exactly what constants enter a model. Naturally, anyone who sets out to verify a calculation by others or uses a model for new applications needs a complete specification of the model, for which a full account of the model constants and their values is an essential part. Also, when different models are compared it is highly valuable to fully understand exactly what constants enter the models. Unfortunately, discussions of model constants are often incomplete, misleading, and/or erroneous. For example, in Table A of Ref. [4] the number of constants of the mass model of Spanier and Johansson [15] is listed as 12. However, in Table A in the article [15] by Spanier and Johansson the authors themselves list 30 constants plus five magic numbers that are not calculated within the mass model and must therefore be considered constants, for a total of at least 35 constants.

We specify in Table I *all* the constants that enter the 1988 version of the FRDM model, rather than just those that in the final step are adjusted to experimental data by a least-squares procedure. We also include fundamental constants like the electronic charge and Planck's constant.

The discussions in Refs. [5,7] allow us to enumerate the constants in the FRDM model in Table I. From this list we see that the macroscopic-microscopic method requires relatively few constants. One feature of the model gives rise to a small complication when counting the number of constants. Droplet-model constants occur also in the determination of the single-particle potential. However, the six droplet-model constants used in the microscopic expressions are obtained from four primary constants [16], one of which is the nuclear radius constant r_0. Since this constant has the same value as we use in our macroscopic model only three remain that could be considered as additional FRDM constants. Alternatively we could in principle employ an iterative procedure and obtain the same values for the macroscopic and microscopic droplet-model constants. In that case the total number of FRDM constants would be 36 and the number of constants adjusted to masslike quantities 15.

III. FERMION DYNAMICAL SYMMETRY MODEL MASS FORMULA

A. Model features and constants

Here we present the principal terms that enter in the *FDSM Strutinsky atomic mass formula*. Our purpose with the brief outline is only that we later be able to identify where in

TABLE I. Constants in the FRDM (1988). The third column gives the number of constants adjusted to nuclear masses or masslike quantities such as odd-even mass differences or fission-barrier heights. The fourth column gives the number of constants determined from other considerations. Appropriate numerical values of the macroscopic constants are given in Ref. [7] and of the microscopic constants in Ref. [5].

Constants	Comment	Masslike	Other
M_H, M_n, e^2	Macroscopic fundamental constants	0	3
a_{el}, r_0, r_p, a, a_{den}, K	Macroscopic constants from considerations other than masslike data	0	6
L, a_3, r, s, t, h	Macroscopic constants obtained in prior adjustments to masslike data	6	0
a_1, a_2, J, Q, a_0, W C, γ, c_a	Macroscopic constants determined by current least-squares adjustments	9	0
$\hbar c$, m_{nuc}	Microscopic fundamental constants	0	2
V_s, V_a, A_{den}, B_{den}, C_{cur}, k_p, l_p, k_n, l_n, a_{pot}	Microscopic constants	0	10
a_1, a_2, J, K, L, Q	Droplet-model constants that enter the single-particle potential	3 [a]	0 [a]
Subtotals		18	21
Total			39

[a]See the discussion of the droplet-model constants in the text.

the mass model various constants enter. For a more extensive presentation we refer to the original work [1].

In the FDSM the nuclear mass is given by $M_{\mathrm{FDSM}}(Z,N)$ with

$$M_{\mathrm{FDSM}}(Z,N)=M_{\mathrm{lq}}^{\mathrm{S}}+M_{\mathrm{sh}}^{\mathrm{s.p.}}+V_{\mathrm{sh}}^{\mathrm{pair}}+\langle V_{\mathrm{FDSM}}\rangle, \tag{2}$$

where $M_{\mathrm{lq}}^{\mathrm{S}}$ is the spherical liquid-drop energy and the remaining three terms account for the shell-plus-pairing corrections.

1. Spherical liquid-drop model

Only the spherical liquid-drop energy is needed in the FDSM model, since other terms are assumed to generate the macroscopic deformation effects that in the macroscopic-microscopic finite-range liquid-drop model are described by a deformed macroscopic energy expression. For generality we give the expression for the deformed case and then specialize to the spherical case. $M_{\mathrm{lq}}^{\mathrm{S}}$ of the FDSM model is identical to the macroscopic FRLDM energy [7] in its spherical limit. Thus

$$\begin{aligned}M_{\mathrm{lq}}^{\mathrm{S}}=&M_H Z+M_n N-a_v(1-\kappa_v I^2)A+a_s(1-\kappa_s I^2)B_1A^{2/3}\\&+c_0A^0+c_1\frac{Z^2}{A^{1/3}}B_3-c_4\frac{Z^{4/3}}{A^{1/3}}+f(k_f r_p)\frac{Z^2}{A}-c_a(N-Z)\\&+W\left(|I|+\begin{cases}1/A, & Z \text{ and } N \text{ odd and equal}\\ 0, & \text{otherwise}\end{cases}\right)\\&+\begin{cases}+\overline{\Delta}_p+\overline{\Delta}_n-\delta_{np}, & Z \text{ and } N \text{ odd}\\ +\overline{\Delta}_p, & Z \text{ odd and } N \text{ even}\\ +\overline{\Delta}_n, & Z \text{ even and } N \text{ odd}\\ +0, & Z \text{ and } N \text{ even}\end{cases}\\&-a_{el}Z^{2.39}\end{aligned} \tag{3}$$

with B_1 and B_3 given by their values in the spherical limit as given by Eq. (13) below. The average neutron pairing gap $\overline{\Delta}_n$ and the average proton pairing gap $\overline{\Delta}_p$ are given by [17,18]

$$\overline{\Delta}_n=\frac{rB_s}{N^{1/3}}e^{-sI-tI^2} \tag{4}$$

and

$$\overline{\Delta}_p=\frac{rB_s}{Z^{1/3}}e^{+sI-tI^2}. \tag{5}$$

The average neutron-proton interaction energy δ_{np} is given by [17,18]

$$\delta_{np}=\frac{h}{B_s A^{2/3}}. \tag{6}$$

In the above expressions the quantities c_1 and c_4 are defined in terms of the electronic charge e and the nuclear-radius constant r_0 by

$$c_1=\frac{3}{5}\frac{e^2}{r_0},$$

$$c_4=c_1\frac{5}{4}\left(\frac{3}{2\pi}\right)^{2/3}. \tag{7}$$

The proton form factor f is given by

$$f(k_f r_p)=-\frac{1}{8}\frac{{r_p}^2e^2}{r_0^3}\left[\frac{145}{48}-\frac{327}{2880}(k_f r_p)^2+\frac{1527}{1209600}(k_f r_p)^4\right], \tag{8}$$

where the Fermi wave number is

$$k_f=\left(\frac{9\pi Z}{4A}\right)^{1/3}\frac{1}{r_0}. \tag{9}$$

The relative neutron excess I is

$$I=\frac{N-Z}{N+Z}. \tag{10}$$

The relative surface energy B_s, which is the ratio of the surface area of the nucleus at the actual shape to the surface area of the nucleus at the spherical shape, is given by

$$B_s=\frac{A^{-2/3}}{4\pi r_0^2}\int_S dS \tag{11}$$

which in the spherical limit is 1. The quantity B_1 represents the relative generalized surface or nuclear energy in a model that accounts for the effect of the finite range of the nuclear force and B_3 is the relative Coulomb energy, including diffuseness corrections to all orders. For spherical shapes one can calculate the quantities B_1 and B_3 analytically. With

$$x_0=\frac{r_0A^{1/3}}{a} \quad \text{and} \quad y_0=\frac{r_0A^{1/3}}{a_{\text{den}}} \tag{12}$$

one obtains

$$B_1=1-\frac{3}{x_0^2}+(1+x_0)\left(2+\frac{3}{x_0}+\frac{3}{x_0^2}\right)e^{-2x_0},$$

$$B_3=1-\frac{5}{y_0^2}\left[1-\frac{15}{8y_0}+\frac{21}{8y_0^3}-\frac{3}{4}\times\left(1+\frac{9}{2y_0}+\frac{7}{y_0^2}+\frac{7}{2y_0^3}\right)e^{-2y_0}\right]. \tag{13}$$

The expression B_3 for the relative Coulomb energy yields the energy for a homogeneously charged, diffuse-surface nucleus to all orders in the diffuseness parameter a_{den}. The constants in front of B_1 and B_3 have been chosen so that B_1 and B_3 are 1 for a sphere in the limit in which the range a and diffuseness a_{den} go to zero, in analogy with the definition of the quantities B_s and B_C in the standard liquid-drop model.

2. Values of the constants of spherical liquid-drop energy

The constants appearing in the expression for the FRLDM macroscopic model fall into three categories [19,20]. The first category, which represents constants that were taken from previous work with no adjustment whatsoever, includes [18–20]

M_H	=	7.289034	MeV	hydrogen-atom mass excess,
M_n	=	8.071431	MeV	neutron mass excess,
e^2	=	1.439 976 4	MeV fm	electronic charge squared,
a_{den}	=	$0.99/2^{1/2}$	fm	range of Yukawa function used to generate nuclear charge distribution,
a_{el}	=	1.433×10^{-5}	MeV	electronic-binding constant,
r	=	5.72	MeV	pre-exponential pairing constant,
s	=	0.118		linear exponential pairing constant,
t	=	8.12		quadratic exponential pairing constant,
h	=	6.82	MeV	neutron-proton interaction constant,
r_p	=	0.80	fm	proton root-mean-square radius.

The second category, representing those constants whose values were determined from considerations other than nuclear ground-state masses, includes [19,20]

r_0	=	1.16	fm	nuclear-radius constant,
a	=	0.68	fm	range of Yukawa-plus-exponential potential,
a_s	=	21.13	MeV	surface-energy constant,
κ_s	=	2.3		surface-asymmetry constant.

The third category represents five constants whose values are determined from a least-squares adjustment to nuclear ground-state masses by Ref. [7]. Their values are

a_v	=	16.000	MeV	volume-energy constant,
κ_v	=	1.911		volume-asymmetry constant,
W	=	35	MeV	Wigner constant,
c_0	=	5.8	MeV	A^0 constant,
c_a	=	0.145	MeV	charge-asymmetry constant.

3. Spherical shell correction

The spherical shell correction $M_{\text{sh}}^{\text{s.p.}}$, term two in Eq. (2), is given by

$$M_{\text{sh}}^{\text{s.p.}}=M_{\text{sh}}^{\text{s.p.}}(Z)+M_{\text{sh}}^{\text{s.p.}}(N)=\sum_{i=83}^{Z}\varepsilon_i^{\pi}n_i^{\pi}-[E_{\text{FG}}(Z)-E_{\text{FG}}(82)]+n_p\varepsilon_p+\sum_{i=127}^{N}\varepsilon_i^{\nu}n_i^{\nu}-[E_{\text{FG}}(N)-E_{\text{FG}}(126)]+n_n\varepsilon_n, \tag{14}$$

where ε_i^{π} and ε_i^{ν} are the proton and neutron single-particle energies and where, in this case, $n_i^{\pi}=1$ and $n_i^{\nu}=1$. Furthermore, $E_{\text{FG}}(n)$ represents the Fermi-gas energy for n nucleons:

$$E_{\rm FG}(Z)=\frac{3Z^{5/3}C_{\rm p}}{5R_{\rm p}{}^2},$$

$$E_{\rm FG}(N)=\frac{3N^{5/3}C_{\rm n}}{5R_{\rm n}{}^2}, \tag{15}$$

and

$$R_{\rm n,p}=r_0A^{1/3}\left[\frac{1\pm I}{(1-3\overline{\epsilon})(1\pm\overline{\delta})}\right]^{1/3} \tag{16}$$

with

$$\overline{\delta}=\left(I+\frac{3}{16}\frac{c_1}{Q}\frac{Z}{A^{2/3}}\right)\Big/\left(1+\frac{9}{4}\frac{J}{Q}\frac{1}{A^{1/3}}\right) \tag{17}$$

and

$$\overline{\epsilon}=\left(-2a_2\frac{1}{A^{1/3}}+L\overline{\delta^2}+c_1\frac{Z^2}{A^{4/3}}\right)/K. \tag{18}$$

The calculation of the spherical shell corrections uses a set of spherical single-particle levels. Thus these levels and their associated l and j quantum numbers, which are needed to provide the parity and degeneracy of the levels constitute constants of the model, as do the spherical magic numbers in the beginning and end of the region. The proton magic numbers are 82 and 126, and the neutron magic numbers are 126 and 184. Between these magic numbers there are six spherical proton and seven spherical neutron levels. Some constants of the model depend on the particular set of single-particle levels used. We give below the set of constants appropriate for the Woods-Saxon single-particle level scheme, used in Refs. [1,6].

The quantities $\varepsilon_{\rm p}$ and $\varepsilon_{\rm n}$ in Eq. (14) represent approximately the differences between the Fermi-gas and the more exact single-particle level schemes represented by the energies ε_i^{π} and ε_i^{ν}. The number of valence nucleons $n_{\rm p}$ and $n_{\rm n}$ are, obviously $n_{\rm p}=Z-82$ and $n_{\rm n}=N-126$. The following definition was chosen for $\varepsilon_{\rm p}$ and $\varepsilon_{\rm n}$:

$$\varepsilon_{\rm p}=\left(\frac{3}{5}83^{5/3}-\frac{3}{5}82^{5/3}\right)C_{\rm p}/R_{\rm p}{}^2+e_{\rm p},$$

$$\varepsilon_{\rm n}=\left(\frac{3}{5}127^{5/3}-\frac{3}{5}126^{5/3}\right)C_{\rm n}/R_{\rm n}{}^2+e_{\rm n}. \tag{19}$$

The quantities $e_{\rm p}$ and $e_{\rm n}$ are determined by requiring the maximum cancellations in Eq. (14), or equivalently by minimizing $\Sigma_{Z=83}^{126}[M_{\rm sh}^{\rm s.p.}(Z)]^2$ and $\Sigma_{N=127}^{184}[M_{\rm sh}^{\rm s.p.}(N)]^2$.

The various terms entering in Eq. (14) are shown in Fig. 1 as functions of the proton number for neutron number $N=126$. The solid curve represents the Fermi-gas energy $E_{\rm FG}(Z)-E_{\rm FG}(82)$ with $E_{\rm FG}(Z)$ defined by Eq. (15) and the short-dashed curve the total sum of single-particle energies $\Sigma_{i=83}^{Z}\varepsilon_i^{\pi}n_i^{\pi}+n_{\rm p}\varepsilon_{\rm p}$. The difference between the two curves defines the spherical shell-correction energy $M_{\rm sh}^{\rm s.p.}$. The contribution from the first term in the single-particle energy is small, corresponding to the long-dashed curve. The main contribution to the sum of single-particle energies comes from $n_{\rm p}\varepsilon_{\rm p}$, with $\varepsilon_{\rm p}$ defined in Eq. (19). For $e_{\rm p}=0$ this term gives a contribution to the energy corresponding to the dot-dashed curve in Fig. 1. Adding to this curve the sum of single-particle energies given by the long-dashed curve results in an energy which is consistently lower than the Fermi-gas energy given by the solid curve. This would result in a spherical shell-correction energy which is negative for all proton numbers. To avoid this, a nonzero value for $e_{\rm p}$ is introduced, resulting in an additional contribution to the total sum of single-particle energies, $n_{\rm p}e_{\rm p}$, shown by the dotted line. Since both the dotted and the dot-dashed curves are smooth functions of the proton number, the only true shell correction must be contained in the long-dashed curve. The other two terms are only introduced to have the total sum of single-particle energies (the short-dashed curve, corresponding to the sum of the long-dashed, dotted and dot-dashed curves) fluctuate around the Fermi-gas energy (the solid curve). However, the difference between the short-dashed and solid curves, defined to represent the ''spherical shell-correction energy,'' does not correspond to what is normally called the shell-correction energy. This will be shown in Sec. IV B below.

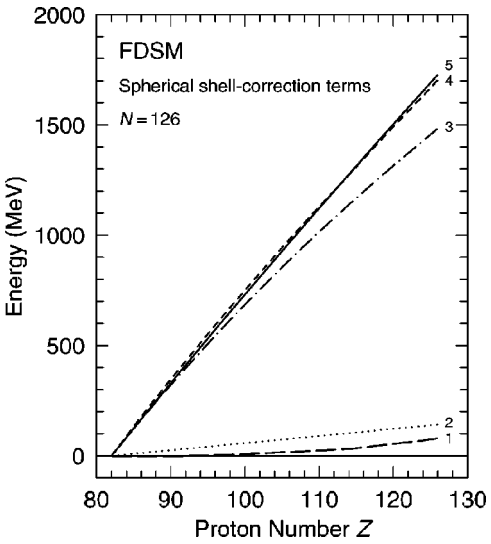

FIG. 1. Terms entering the expression for the spherical proton shell-correction energy $M_{\rm sh}^{\rm s.p.}(Z)$. Curve 1 shows $\Sigma_{i=83}^{Z}\varepsilon_i^{\pi}n_i^{\pi}$. Curve 2 shows $n_{\rm p}e_{\rm p}$. Curve 3 shows $n_{\rm p}(\frac{3}{5}83^{5/3}-\frac{3}{5}82^{5/3})C_{\rm p}/R_{\rm p}{}^2=n_{\rm p}(\varepsilon_{\rm p}-e_{\rm p})$. Curve 4 is the sum of the curves 1, 2, and 3. Curve 5 shows $E_{\rm FG}(Z)-E_{\rm FG}(82)$. The spherical proton shell correction $M_{\rm sh}^{\rm s.p.}(Z)$ is given by the difference between the curves 4 and 5.

4. Values of the constants of the spherical shell correction

The constants of the spherical shell correction are

J	=	38.2	MeV	symmetry-energy constant,
L	=	100.0	MeV	density-energy constant,
c_1	=	0.7403	MeV	Coulomb-energy constant,
K	=	300	MeV	nuclear compressibility constant,

TABLE II. Woods-Saxon single-particle level energies and quantum numbers used in the FDSM.

Protons			Neutrons		
Energy (MeV)	l	j	Energy (MeV)	l	j
5.099	p	1/2	3.808	d	3/2
3.880	f	5/2	3.452	s	1/2
3.850	p	3/2	2.950	g	7/2
1.684	i	13/2	2.355	d	5/2
0.921	f	7/2	1.201	j	15/2
0.000	h	9/2	0.665	i	11/2
			0.000	g	9/2

$a_2 = 20.85$ MeV surface-energy constant,
$Q = 17.7$ MeV effective surface-stiffness constant,
$C_\mathrm{p} = 72$ MeV proton Fermi-energy constant,
$C_\mathrm{n} = 71$ MeV neutron Fermi-energy constant,
$e_\mathrm{p} = 3.212$ MeV proton scaling constant,
$e_\mathrm{n} = 3.477$ MeV neutron scaling constant.

The spherical Woods-Saxon proton and neutron single-particle levels and quantum numbers used in the FDSM are shown in Table II.

5. Spherical pairing correction

The spherical pairing correction $V_{\mathrm{sh}}^{\mathrm{pair}}$, term three in Eq. (2), is given by

$$V_{\mathrm{sh}}^{\mathrm{pair}}=[V_{\pi}^{\mathrm{pair}}(\mathrm{BCS})-V_{\pi}^{\mathrm{pair}}(\mathrm{deg})]+[V_{\nu}^{\mathrm{pair}}(\mathrm{BCS})-V_{\nu}^{\mathrm{pair}}(\mathrm{deg})]. \tag{20}$$

In Eq. (20) $V_{\sigma}^{\mathrm{pair}}(\mathrm{BCS})$ is the pairing energy obtained from a given single-particle level scheme by solving the standard BCS equations ($\sigma=\pi,\nu$). The pairing energy $V_{\sigma}^{\mathrm{pair}}(\mathrm{deg})$ for a degenerate level scheme may be determined analytically:

$$V_{\sigma}^{\mathrm{pair}}(\mathrm{deg})=G_{\sigma}N^{\sigma}(\Omega^{\sigma}-N^{\sigma}+N^{\sigma}/\Omega^{\sigma})(\sigma=\pi,\nu). \tag{21}$$

The symbol Ω denotes the shell degeneracy. In the presentation of the FDSM model it is stated that the BCS approximation is used here only to calculate the corrections due to the spherical single-particle splitting and that the principle part of the pairing in the FDSM is treated below as a two-body interaction.

It should be observed that the BCS pairing energy, $V_{\pi}^{\mathrm{pair}}(\mathrm{BCS})$ does not fluctuate around the pairing energy for the degenerate level scheme, $V_{\pi}^{\mathrm{pair}}(\mathrm{deg})$. Both energies are negative, but for nearly all nuclei $V_{\pi}^{\mathrm{pair}}(\mathrm{deg})$ has a much larger negative value than $V_{\pi}^{\mathrm{pair}}(\mathrm{BCS})$, resulting in positive values of $V_{\mathrm{sh}}^{\mathrm{pair}}$ for the large majority of nuclei. The situation is illustrated for the $N=126$ isotones in Fig. 2. The downsloping trend of $V_{\mathrm{sh}}^{\mathrm{pair}}$ is the result of having included a term $-G\Sigma_i v_i^4$ in the pairing energy.

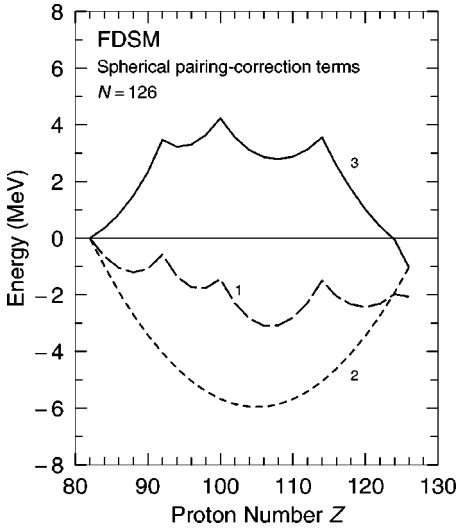

FIG. 2. Terms appearing in the spherical pairing correction energy $V_{\mathrm{sh}}^{\mathrm{pair}}$. Curve 1 shows $V_{\pi}^{\mathrm{pair}}(\mathrm{BCS})$. Curve 2 shows $V_{\pi}^{\mathrm{pair}}(\mathrm{deg})$. The spherical proton pairing correction $V_{\mathrm{sh}}^{\mathrm{pair}}(Z)$ is given by the difference between curve 1 and curve 2 and shown by curve 3.

6. Values of the constants of the spherical pairing correction

The constants of the spherical pairing correction are, for the case of Woods-Saxon levels

$G_{\pi}^{\mathrm{pair}} = -0.094$ MeV pairing strength constant for protons, WS levels,
$G_{\nu}^{\mathrm{pair}} = -0.052$ MeV pairing strength constant for neutrons, WS levels,
$G_{\pi} = -0.047$ MeV pairing strength constant for protons, deg. levels,
$G_{\nu} = -0.023$ MeV pairing strength constant for neutrons, deg. levels.

7. The FDSM shell-correction term $\langle V_{FDSM}\rangle$

In Ref. [1] it is shown that in the symmetry limits

$$\begin{aligned}\langle V_{\mathrm{FDSM}}\rangle=&a_{\alpha}+b_{\alpha}N_{\mathrm{p}}+c_{\alpha}N_{\mathrm{p}}{}^2+d_{\alpha}N_{\mathrm{n}}+e_{\alpha}N_{\mathrm{n}}{}^2+f_{\alpha}N_{\mathrm{p}}N_{\mathrm{n}}\\&+B_2^{\pi\nu}\langle\mathbf{V}_{\mathrm{Q}}^{\pi\nu}\rangle_{\alpha}+G_2^{\pi}\langle\Delta\mathbf{C}_{\mathrm{Sp6}}^{\pi}\rangle_{\alpha}+G_2^{\nu}\langle\Delta\mathbf{C}_{\mathrm{Sp6}}^{\nu}\rangle_{\alpha}\\&+\mathcal{G}_0^{\pi}\langle\Delta\mathbf{C}_{SU2}^{\pi}\rangle_{\alpha}+\mathcal{G}_0^{\nu}\langle\Delta\mathbf{C}_{SU2}^{\nu}\rangle_{\alpha}+(G_0^{\pi}-G_2^{\pi})\\&\times\langle\Delta\mathbf{C}_{\mathrm{SU2}}^{\pi}\rangle_{\alpha}+(G_0^{\nu}-G_2^{\nu})\langle\Delta\mathbf{C}_{\mathrm{SU2}}^{\nu}\rangle_{\alpha}\\&+(B_2^{\pi}-G_2^{\pi})\langle\Delta\mathbf{C}_{\mathrm{SU3}}^{\pi}\rangle_{\alpha}+(B_2^{\nu}-G_2^{\nu})\\&\times\langle\Delta\mathbf{C}_{\mathrm{SU3}}^{\nu}\rangle_{\alpha}\quad(\alpha=\mathrm{SU}_2,\mathrm{SU}_3).\end{aligned} \tag{22}$$

In Eq. (22) N_{p} and N_{n} are the pair numbers of valence protons and neutrons respectively; the expectation values of the operators inside $\langle\rangle$ are discussed in Ref. [1]. The remaining quantities are constants whose values are given below.

8. Values of the constants of $\langle V_{FDSM}\rangle$

The constants of the FDSM shell correction fall into two categories. The constants of the first category, which repre-

TABLE III. Constants of the FDSM. Constants that have not been obtained from adjustments to masslike data, such as nuclear masses, fission barriers, or odd-even mass differences are enclosed in brackets. The number in () in the comment column refers to the more extensive comments in the text. The third column gives the number of constants adjusted to nuclear masses or masslike quantities such as odd-even mass differences. The fourth column gives the number of constants determined from other considerations.

Constants	Comment	Masslike	Other
(82),(126),(126),(184)	Spherical magic numbers (1)	0	4 [b]
$J,L,(c_1),(K),a_2,Q,$ e_p [a], e_n [a], $(C_p),(C_n)$	Fermi-gas par. (2)	4	4
$G_\pi^{pair},G_\nu^{pair},G_\pi$ [a], G_ν [a]	Spherical pairing constants (3)	2	0
$(M_H),(M_n),a_v,a_s,(a_{den}),$ $\kappa_v,\kappa_s,c_0,(a),c_a,W,$ $(a_{el}),h,(r_0),(r_p)$	M^S_{lq} spher. liq.-drop par. (4)	8	7
$G_0^\pi,G_0^\nu,G_2^\pi,G_2^\nu,\ B_2^\pi,\ B_2^\nu$	V_{FDSM} pairing par., norm. (5)	6	0
$\mathcal{G}_0^\pi,\mathcal{G}_0^\nu$	V_{FDSM} pairing par., abnorm. (6)	2	0
$a_\alpha,b_\alpha,c_\alpha,d_\alpha,e_\alpha,f_\alpha$	V_{FDSM} par., $\alpha=$SU2 (7)	6	0
$a_\alpha,b_\alpha,c_\alpha,d_\alpha,e_\alpha,f_\alpha$	V_{FDSM} par., $\alpha=$SU3 (8)	6	0
$B_2^{\pi\nu}$	V_{FDSM} par. (9)	1	0
$(\varepsilon_i^\pi),\ (\varepsilon_i^\nu)$	13 spherical levels, assoc. l and j (10)	0	37[b]
Subtotals		35	54[b]
Total			87[b]

[a]These constants are determined from a least-squares minimization and are therefore not counted as constants of the model.

[b]The number given is appropriate when experimental level energies are used. When Woods-Saxon levels are used the 39 level energies and spins are determined from an underlying model whose number of constants is smaller, perhaps about 15, as in the FRDM microscopic model. Because the lowest single-particle level is renormalized to 0.0 for both neutrons and protons in the FDSM we reduce the number of level energies and spins from 39 to 37 in the table.

sents the nonpairing part, were determined directly from a least-squares adjustment to nuclear masses. For $\alpha=$SU(2) the constant values are:

$$
\begin{aligned}
a_\alpha &= -13.7500 \text{ MeV},\\
b_\alpha &= -4.5720 \text{ MeV},\\
c_\alpha &= 0.4293 \text{ MeV},\\
d_\alpha &= -4.8890 \text{ MeV},\\
e_\alpha &= 0.3306 \text{ MeV},\\
f_\alpha &= -0.2915 \text{ MeV},\\
B_2^{\pi\nu} &= -0.0912 \text{ MeV},
\end{aligned}
$$

and for $\alpha=$SU(3)

$$
\begin{aligned}
a_\alpha &= -5.5700 \text{ MeV},\\
b_\alpha &= -5.7900 \text{ MeV},\\
c_\alpha &= 0.3713 \text{ MeV},\\
d_\alpha &= -6.8060 \text{ MeV},\\
e_\alpha &= 0.3587 \text{ MeV},\\
f_\alpha &= -0.1095 \text{ MeV},\\
B_2^{\pi\nu} &= -0.0912 \text{ MeV}.
\end{aligned}
$$

The second category consists of constants that enter into the pairing part of $\langle V_{FDSM}\rangle$ and were determined from adjustments to odd-even mass differences:

$$
\begin{aligned}
G_0^\pi &= -0.142 \text{ MeV},\\
G_2^\pi &= -0.064 \text{ MeV},\\
B_2^\pi &\approx 0 \text{ MeV},\\
G_0^\nu &= -0.082 \text{ MeV},\\
G_2^\nu &= -0.044 \text{ MeV},\\
B_2^\nu &\approx 0 \text{ MeV},\\
\mathcal{G}_0^\pi &= -0.200 \text{ MeV},\\
\mathcal{G}_2^\nu &= -0.150 \text{ MeV}.
\end{aligned}
$$

B. Constants of the FDSM

The constants that enter in the FDSM are listed in Table III. By constants we mean numbers used in the mass formula, that cannot be (or have not been) derived from the FDSM model itself. Instead, they are taken from other sources or obtained from adjustments to data, including nuclear masses. In addition to the very brief comments in the table one should observe the following:

(1) The magic numbers used in the FDSM have been obtained from a single-particle model.

(2) Most of the Fermi-gas constants are droplet model constants. Most of the constants of the droplet model [21,22]

are determined from least-squares adjustment to masses and fission barriers.

(3) The spherical pairing constants are deduced from odd-even mass differences.

(4) The spherical liquid-drop constants have been taken from the work of Möller and Nix [7,23]. These authors obtained the constants from adjustments to masses, fission barriers, and other considerations.

(5) These constants enter the pairing part of the FDSM shell-correction term V_{FDSM} and have been determined from considerations of odd-even mass differences. The constants are valid if the odd nucleon is in a normal parity level.

(6) These constants enter the pairing part of the FDSM shell-correction term V_{FDSM} and have been determined from considerations of odd-even mass differences. The constants are valid if the odd nucleon is in an abnormal parity level.

(7) Constants of the FDSM shell-correction term V_{FDSM} for $\alpha=\mathrm{SU}(2)$. The constants have been determined from adjustments to experimental nuclear masses.

(8) Constants of the FDSM shell-correction term V_{FDSM} for $\alpha=\mathrm{SU}(3)$. The constants have been determined from adjustments to experimental nuclear masses.

(9) Constant of the FDSM shell-correction term V_{FDSM}. The constant has been determined from adjustments to experimental nuclear masses.

(10) Spherical single-particle level energies with associated spins and angular momentum values have to be available as input to the FDSM mass calculation. This corresponds to $3\times 13=39$ constants.

The above list of the constants should be compared to the claim of the authors of the FDSM paper: *''Thus we have reduced the number of adjustable parameters in the FDSM-Strutinsky mass formula from 16 in version I to 13 in version II.''*

This statement is only correct in the sense that in *the final step of parameter adjustment* only 13 constants [corresponding to (7), (8), and (9) in Table III] were varied. However, at that point the authors had already adjusted the value of the constants on lines (3), (5), and (6) in Table III and still other constants are fitted to masslike data, although the authors of the FDSM paper did not themselves specifically adjust those values for their mass calculations but took them from other sources. Finally, it should be mentioned that the number of mass-related constants (as well as the total number of constants) is considerably smaller in version I of the FDSM mass formula. In version I of the FDSM there are in total 19 constants of which seven are SU(2) constants, nine are SU(3) constants and three are common constants for the two symmetries, namely the mass of ^{208}Pb, the proton mass and the neutron mass. The seven SU(2) and nine SU(3) constants are all fitted in the FDSM version I.

IV. AN EVALUATION OF THE FDSM MASS FORMULA

A. ''Experimental'' data set used in adjustment

The FDSM discussed here has been applied only to the calculation of actinide masses. The authors of Ref. [1] state *''These 13 parameters are determined by adjustment to 332 known actinide-region masses.''*

Since there were only 246 measured masses available for $Z\geqslant 82$, in the latest compilation at about the time the FDSM constants were fitted, namely in the 1989 Audi interim table [24], it is clear that the authors have made the mistake of including masses given by ''Wapstra systematics.'' These are masses that have not been measured. Instead, they have been calculated by Wapstra [25] by means of extrapolation from known masses. Thus the authors have, partially, adjusted their model to another model. We have investigated the error associated with the ''Wapstra systematics'' model. From a 1977 mass table [26,27] we have selected the masses given by the Wapstra systematics for which real measurements were given in the 1989 Audi interim table [24]. There were in all 253 such masses in all regions of nuclei. These 253 new measurements were usually close to previously known masses. The rms error between the systematics masses and these new masses was 0.45 MeV.

B. FDSM ''Strutinsky-like shell correction''

The method used in the FDSM for calculating the ''Strutinsky-like shell correction'' is definitely not Strutinsky-like. In fact, it is contrary to all the ideas introduced by Strutinsky and is actually more similar to the pre-Strutinsky method of just summing single-particle level energies. The method is therefore fraught with all the problems associated with that, now abandoned, method.

In order to make a physical interpretation of the Strutinsky-like shell correction $M_{\mathrm{sh}}^{\mathrm{s.p.}}$ used in the FDSM we rewrite Eq. (14) in the following way:

$$
\begin{aligned}
M_{\mathrm{sh}}^{\mathrm{s.p.}}=&\left\{\sum_{i=83}^{Z}(\varepsilon_i^{\pi}+\varepsilon_{\mathrm{p}})n_i^{\pi}+\sum_{i=1}^{82}(\varepsilon_i^{\pi}+\varepsilon_{\mathrm{p}})n_i^{\pi}-E_{\mathrm{smo}}(Z)\right\}\\
&+\{E_{\mathrm{smo}}(Z)-E_{\mathrm{FG}}(Z)\}-\{E_{\mathrm{smo}}(82)-E_{\mathrm{FG}}(82)\}\\
&-\left\{\sum_{i=1}^{82}(\varepsilon_i^{\pi}+\varepsilon_{\mathrm{p}})n_i^{\pi}-E_{\mathrm{smo}}(82)\right\}\\
&+\text{corresponding terms for neutrons.}
\end{aligned}
\tag{23}
$$

We have here introduced the true smooth Strutinsky energy E_{smo}, which has to be calculated from the full set of single-particle energies through the Strutinsky smearing procedure. In the FDSM mass formula, these energies are only defined for $82<Z\leqslant 126$ (and for neutrons for $126<N\leqslant 184$), but this has no consequence for the above formula, since each term which depends on the single-particle energies outside these intervals and are added in the formula is also subtracted out. Therefore the expression for $M_{\mathrm{sh}}^{\mathrm{s.p.}}$ given in Eqs. (14) and (23) are identical. In Eq. (23), the various terms have been ordered into groups enclosed by brackets. The first group of terms is identical to the true Strutinsky shell-correction energy $E_{\mathrm{shell}}(Z)$, provided that $E_{\mathrm{smo}}(Z)$ is calculated from the renormalized single-particle energies $\varepsilon_i^{\pi}+\varepsilon_{\mathrm{p}}$. The value of ε_{p} does then not effect $E_{\mathrm{shell}}(Z)$, since it will cancel out exactly. The second group of terms gives the difference between the smooth Strutinsky energy and the Fermi-gas energy for proton number Z. From now on we will use the

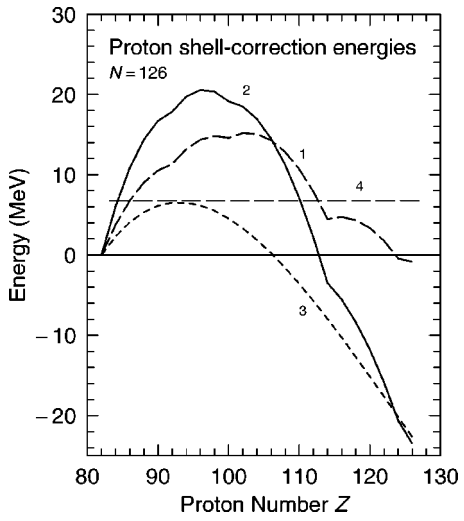

FIG. 3. The true Strutinsky shell-correction energy for protons, $E^{\pi}_{\rm shell}(Z)$, calculated from the Woods-Saxon single-particle level energies is shown by curve 1. A constant term, shown by curve 4, has been added to $E^{\pi}_{\rm shell}(Z)$ in order to normalize the energy to zero for $Z=82$. The proton part of the spherical shell-correction energy of the FDSM, $M^{\rm s.p.}_{\rm sh}(Z)$, is shown by curve 2. Curve 3 shows the difference between curve 2 and curve 1. It represents a smooth energy of macroscopic origin, $E^{\pi}_{\rm smo\text{-}FG}(Z)-E^{\pi}_{\rm smo\text{-}FG}(82)$, contained in the FDSM spherical shell-correction energy, cf. Eq. (24).

notation $E_{\rm smo\text{-}FG}(Z)$ for this term. The third group of terms is defined in the same way as the second group but for proton number $Z=82$ and can therefore be written as $E_{\rm smo\text{-}FG}(82)$. Finally, the fourth group of terms is identical to the true Strutinsky shell-correction energy for proton number 82, i.e., $E_{\rm shell}(82)$. We can now rewrite Eq. (14) as

$$\begin{aligned} M^{\rm s.p.}_{\rm sh} = & E^{\pi}_{\rm shell}(Z)+E^{\pi}_{\rm smo\text{-}FG}(Z)-E^{\pi}_{\rm smo\text{-}FG}(82) \\ & -E^{\pi}_{\rm shell}(82)+E^{\nu}_{\rm shell}(N)+E^{\nu}_{\rm smo\text{-}FG}(N) \\ & -E^{\nu}_{\rm smo\text{-}FG}(126)-E^{\nu}_{\rm shell}(126), \end{aligned} \tag{24}$$

where we have written out explicitly also the neutron terms. By adding the proton and neutron terms we finally get

$$\begin{aligned} M^{\rm s.p.}_{\rm sh} = & E_{\rm shell}(Z,N)+E_{\rm smo\text{-}FG}(Z,N) \\ & -E_{\rm smo\text{-}FG}(^{208}{\rm Pb})-E_{\rm shell}(^{208}{\rm Pb}). \end{aligned} \tag{25}$$

We can now make a precise interpretation of the ''spherical Strutinsky-like shell-correction energy.'' It is identical to the normal Strutinsky shell energy to which has been added the energy difference between the smooth Strutinsky energy and the Fermi-gas energy, the whole expression normalized to zero for ^{208}Pb. In Fig. 3 the spherical Strutinsky-like shell-correction energy has been split up into these two components. It can then be seen that the normal Strutinsky shell-correction energy and the component corresponding to the energy difference between the smooth Strutinsky energy and the Fermi-gas energy are of the same magnitude.

It is very satisfactory to observe that $M^{\rm s.p.}_{\rm sh}$ indeed contains the true Strutinsky shell-correction energy, $E_{\rm shell}(Z,N)$. On the other hand it is very disturbing to see that also $E_{\rm smo\text{-}FG}(Z,N)$ is contained in $M^{\rm s.p.}_{\rm sh}$, since this term is the difference between two macroscopic energies, namely the smooth Strutinsky energy and the Fermi-gas energy, and therefore macroscopic in character. It will therefore vary smoothly with N and Z and not have the oscillating behavior that we associate with a shell energy. Furthermore, the term will become very large at some distance from ^{208}Pb, the nucleus for which it is renormalized to zero by the subtraction of $E_{\rm smo\text{-}FG}(^{208}{\rm Pb})$. Even more serious is that it contains the smooth Strutinsky energy, which is nothing but the smoothed out version of the unphysical sum of single-particle energies. Therefore $M^{\rm s.p.}_{\rm sh}$ has all the deficiencies associated with the pre-Strutinsky era sums of single-particle energies. This cannot be cured by the subtraction of the dropletlike, and therefore in principle physically correct, Fermi-gas energy. On the contrary, by doing so, it is guaranteed that parts of the smooth Strutinsky energy that have an incorrect mass number dependence remain in $M^{\rm s.p.}_{\rm sh}$. However, the FDSM mass formula offers other terms to compensate for this mistake, as we will see later. Finally, to renormalize the shell energy to zero for ^{208}Pb seems very strange, since this is one of the most strongly bound nuclei and therefore traditionally associated with a large negative shell energy, i.e., it has a much lower energy than predicted by the liquid-drop formula. However, also in this case, the FDSM mass formula offers means for compensation as we will discuss in Sec. IV C.

C. FDSM masses for spherical nuclei

It is now possible to make a direct comparison between the macroscopic-microscopic model and the FDSM for spherical nuclei. In the FDSM the nuclear mass is given by Eq. (2). By using the expression for $M^{\rm s.p.}_{\rm sh}$ given in Eq. (25), Eq. (2) can be rewritten as

$$\begin{aligned} M_{\rm FDSM}(Z,N) = & M^{\rm S}_{\rm lq}+E_{\rm shell}(Z,N)+V^{\rm pair}_{\rm sh}(Z,N) \\ & +E_{\rm smo\text{-}FG}(Z,N)-E_{\rm shell}(^{208}{\rm Pb}) \\ & -E_{\rm smo\text{-}FG}(^{208}{\rm Pb})+\langle V_{\rm FDSM}\rangle. \end{aligned} \tag{26}$$

The corresponding expression in the macroscopic-microscopic model is

$$M_{\rm mm}(Z,N)=M^{\rm S}_{\rm lq}(Z,N)+E_{\rm shell}(Z,N)+V^{\rm pair}_{\rm mm}(Z,N). \tag{27}$$

Provided that the same macroscopic energy and the same single-particle energies are used in both models, $M^{\rm S}_{\rm lq}$ and $E_{\rm shell}(Z,N)$ are identical in Eqs. (26) and (27).

By introducing

$$\delta E_{\rm diff}(Z,N)=M_{\rm FDSM}(Z,N)-M_{\rm mm}(Z,N) \tag{28}$$

we get by subtracting Eq. (27) from Eq. (26) and rearranging the terms

$$\langle V_{\mathrm{FDSM}}\rangle = E_{\mathrm{shell}}(^{208}\mathrm{Pb}) + E_{\mathrm{smo\text{-}FG}}(^{208}\mathrm{Pb}) - E_{\mathrm{smo\text{-}FG}}(Z,N) + V_{\mathrm{mm}}^{\mathrm{pair}}(Z,N) - V_{\mathrm{sh}}^{\mathrm{pair}}(Z,N) + \delta E_{\mathrm{diff}}(Z,N). \quad (29)$$

Provided that $\delta E_{\mathrm{diff}}(Z,N)$ is small enough to be neglected, as it in fact is for most nuclei included in the fit, it is straightforward to interpret the meaning of $\langle V_{\mathrm{FDSM}}\rangle$. It consists of two terms related to the nucleus ^{208}Pb, namely the true Strutinsky shell energy and the difference between the smooth Strutinsky energy and the Fermi-gas energy. From this is subtracted two terms related to the nucleus under consideration: the difference between the smooth Strutinsky energy and the Fermi-gas energy and the difference between the spherical pairing correction term of the FDSM mass formula and the pairing correction of the macroscopic-microscopic model, taken at the actual deformation. This interpretation is correct to the order of 1 MeV, which is the size of $\delta E_{\mathrm{diff}}(Z,N)$.

The implication of Eq. (26) is very interesting. Since the nuclear mass is already given to a very good approximation by the three first terms $M_{\mathrm{lq}}^{\mathrm{S}} + E_{\mathrm{shell}}(Z,N) + V_{\mathrm{sh}}^{\mathrm{pair}}(Z,N)$ of Eq. (26), the sum of the remaining terms must add up to only a couple of MeV. However, for nuclei at some distance from ^{208}Pb, the expression $E_{\mathrm{smo\text{-}FG}}(Z,N) - E_{\mathrm{shell}}(^{208}\mathrm{Pb}) - E_{\mathrm{smo\text{-}FG}}(^{208}\mathrm{Pb})$ constituting terms four to six of Eq. (26) is much larger than that. Correct masses can only be obtained if the terms $E_{\mathrm{smo\text{-}FG}}(Z,N) - E_{\mathrm{shell}}(^{208}\mathrm{Pb}) - E_{\mathrm{smo\text{-}FG}}(^{208}\mathrm{Pb})$ are nearly exactly canceled out by $\langle V_{\mathrm{FDSM}}\rangle$ in Eq. (26). That this near cancellation occurs is more clearly seen in the expression for $\langle V_{\mathrm{FDSM}}\rangle$ given in Eq. (29). In addition to the three terms already mentioned, $\langle V_{\mathrm{FDSM}}\rangle$ contains three more terms. The first two are $V_{\mathrm{mm}}^{\mathrm{pair}}(Z,N) - V_{\mathrm{sh}}^{\mathrm{pair}}(Z,N)$, implying that $V_{\mathrm{sh}}^{\mathrm{pair}}(Z,N)$ in Eq. (26) de facto is replaced by the pairing energy of the macroscopic-microscopic model. This replacement is essential, since $V_{\mathrm{mm}}^{\mathrm{pair}}(Z,N) - V_{\mathrm{sh}}^{\mathrm{pair}}(Z,N)$ may amount to several MeV, as illustrated in Fig. 4. The main contribution to the discrepancy comes from V_{π}^{pair}(deg), cf. Fig. 2. The only remaining term in Eq. (29) is $\delta E_{\mathrm{diff}}(Z,N)$, which is typically of the order 1 MeV for nuclei with known masses. It is the only FDSM-related term in which an improvement over the macroscopic-microscopic model can be incorporated in the FDSM mass formula.

In the FDSM paper, $\langle V_{\mathrm{FDSM}}\rangle$ is characterized as the FDSM shell correction. Furthermore, it is stated that it can be obtained by computing the expectation value of the FDSM effective interaction. In reality this is not done, since this term is determined by parameter adjustment to data. Eq. (29), however, leads to a totally different interpretation of $\langle V_{\mathrm{FDSM}}\rangle$. The bulk part of this term serves the single purpose of cancelling out the inappropriate terms in the mass formula of Eq. (26). Its value depends crucially on the microscopic model, mainly through E_{smo}, and on the Fermi-gas model. Any change in the choice of these models or their constant values will therefore alter the value of $\langle V_{\mathrm{FDSM}}\rangle$. Consequently, $\langle V_{\mathrm{FDSM}}\rangle$ is not reflecting properties of the FDSM model and its value cannot be independently calculated from the FDSM effective interaction. In the FDSM mass formula it serves the mere purpose of providing a set of adjustable constants which are used for fitting the ''experimental'' masses.

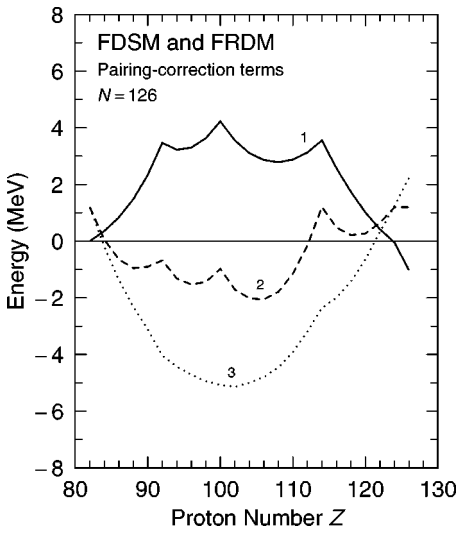

FIG. 4. Curve 1 shows the FDSM spherical proton pairing correction energy, $V_{\mathrm{sh}}^{\mathrm{pair}}(Z)$. Curve 2 shows the proton pairing correction energy of the microscopic-macroscopic model, $V_{\mathrm{mm}}^{\mathrm{pair}}(Z)$. It has in this case been calculated from the same Woods-Saxon level energies as used in the FDSM, but with the standard pairing strength [39], which is somewhat larger than the one used in the FDSM. No term $-G\Sigma_i v_i^4$ is included in $V_{\mathrm{mm}}^{\mathrm{pair}}(Z)$. A smooth energy of -1.2 MeV has been subtracted. Curve 3 shows the difference between curve 2 and curve 1.

In Fig. 5 $\langle V_{\mathrm{FDSM}}\rangle$ is plotted for the $N=126$ isotones (the solid curve). According to the predictions of Eq. (29) it should very closely follow the long-dashed curve, which shows $E_{\mathrm{shell}}(^{208}\mathrm{Pb}) + E_{\mathrm{smo\text{-}FG}}(^{208}\mathrm{Pb}) - E_{\mathrm{smo\text{-}FG}}(Z,N) + V_{\mathrm{mm}}^{\mathrm{pair}}(Z,N) - V_{\mathrm{sh}}^{\mathrm{pair}}(Z,N)$. However, this is only true for proton numbers up to 91, which is the range in which the FDSM constants have been fitted to masses for the $N=126$ isotones. For larger proton numbers, for which no masses are available, the two curves start to deviate. As Z approaches 126 the discrepancies become very large.

For ^{208}Pb Eq. (29) reduces to

$$\langle V_{\mathrm{FDSM}}\rangle_{^{208}\mathrm{Pb}} = E_{\mathrm{shell}}(^{208}\mathrm{Pb}) + V_{\mathrm{mm}}^{\mathrm{pair}}(^{208}\mathrm{Pb}) - V_{\mathrm{sh}}^{\mathrm{pair}}(^{208}\mathrm{Pb}) + \delta E_{\mathrm{diff}}(^{208}\mathrm{Pb}). \quad (30)$$

For this nucleus the pairing terms are small and to the extent that the difference between the two models can be neglected, $\langle V_{\mathrm{FDSM}}\rangle_{^{208}\mathrm{Pb}}$ is simply the Strutinsky shell-correction energy.

D. FDSM masses for deformed nuclei

For deformed nuclei, the total mass can be written as the mass of the nucleus at spherical shape plus a correction due to deformation. This correction must lower the mass, since otherwise the nucleus would be spherical. In the macroscopic-microscopic model the separation into a deformation-independent part and a deformation-dependent part can be written

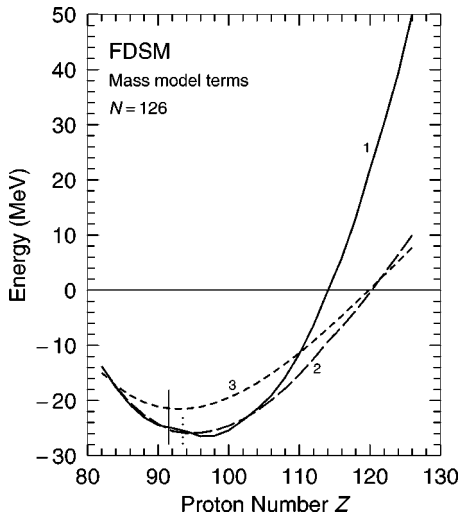

FIG. 5. The FDSM shell correction $\langle V_{\rm FDSM}\rangle$ is shown by curve 1. Curve 2 shows the energy $E_{\rm shell}(^{208}{\rm Pb})+E_{\rm smo\text{-}FG}(^{208}{\rm Pb})-E_{\rm smo\text{-}FG}(Z,N)+V_{\rm mm}^{\rm pair}(Z,N)-V_{\rm sh}^{\rm pair}(Z,N)$, where $V_{\rm mm}^{\rm pair}(Z,N)$ has been calculated in the same way as in Fig. 4. When the FDSM gives the same mass as the microscopic-macroscopic model, the two curves coincide. This is well fulfilled for proton numbers below 92 (i.e., to the left of the vertical solid line), where the FDSM constants have been fitted to known masses. The inclusion of the pairing terms, $V_{\rm mm}^{\rm pair}(Z,N)-V_{\rm sh}^{\rm pair}(Z,N)$, is essential. Putting these terms to zero gives the result shown by curve 3. In the FDSM, SU(3) symmetry is used to the right and SU(2) symmetry to the left of the vertical dotted line.

$$\begin{aligned}M_{\rm mm}(\bar{\beta},Z,N)&=M_{\rm lq}(\bar{\beta},Z,N)+E_{\rm shell}(\bar{\beta},Z,N)+V_{\rm mm}^{\rm pair}(\bar{\beta},Z,N)\\&=M_{\rm lq}^{\rm S}(Z,N)+[M_{\rm lq}(\bar{\beta},Z,N)-M_{\rm lq}^{\rm S}(Z,N)]\\&\quad+E_{\rm shell}^{\rm S}(Z,N)+[E_{\rm shell}(\bar{\beta},Z,N)\\&\quad-E_{\rm shell}^{\rm S}(Z,N)]+V_{\rm mm}^{\rm pair}(0,Z,N)\\&\quad+[V_{\rm mm}^{\rm pair}(\bar{\beta},Z,N)-V_{\rm mm}^{\rm pair}(0,Z,N)].\end{aligned}\tag{31}$$

Here $\bar{\beta}$ denotes a general nonspherical deformation, whereas a superscript S denotes spherical shape. The pairing energy calculated at spherical shape is denoted $V_{\rm mm}^{\rm pair}(0,Z,N)$. The spherical terms are identical to those in Eq. (27), although the notation differs slightly. The sum of the terms in square brackets gives the deformation energy $E_{\rm def}(\bar{\beta},Z,N)$. Equation (31) can then be simplified to

$$\begin{aligned}M_{\rm mm}(\bar{\beta},Z,N)&=M_{\rm lq}^{\rm S}(Z,N)+E_{\rm shell}^{\rm S}(Z,N)+V_{\rm mm}^{\rm pair}(0,Z,N)\\&\quad+E_{\rm def}(\bar{\beta},Z,N)\\&=M_{\rm mm}^{\rm S}(Z,N)+E_{\rm def}(\bar{\beta},Z,N),\end{aligned}\tag{32}$$

where $M_{\rm mm}^{\rm S}(Z,N)$ is the mass calculated for spherical shape.

The FDSM mass formula has the same form for spherical and deformed nuclei. Consequently, in analogy with Eq. (29), we obtain $\langle V_{\rm FDSM}\rangle$ in the deformed case by subtracting Eq. (32) from Eq. (26) and rearranging the terms, with the result

$$\begin{aligned}\langle V_{\rm FDSM}\rangle&=E_{\rm shell}^{\rm S}(^{208}{\rm Pb})+E_{\rm smo\text{-}FG}(^{208}{\rm Pb})-E_{\rm smo\text{-}FG}(Z,N)\\&\quad+V_{\rm mm}^{\rm pair}(0,Z,N)-V_{\rm sh}^{\rm pair}(Z,N)+E_{\rm def}(\bar{\beta},Z,N)\\&\quad+\delta E_{\rm diff}(Z,N)\end{aligned}\tag{33}$$

implying that the full deformation-dependent part of the nuclear mass is contained in $\langle V_{\rm FDSM}\rangle$, which is also what the authors of Ref. [1] claim is the case. Note that Eq. (33) is identical to Eq. (29), except for the inclusion of the deformation-dependent term $E_{\rm def}(\bar{\beta},Z,N)$.

In most macroscopic-microscopic calculations, the energy is not divided as in Eq. (32), but is instead split into a spherical liquid-drop energy and a so-called microscopic correction, $E_{\rm corr}(\bar{\beta},Z,N)$, which contains all shell, pairing, and deformation effects. Thus

$$M_{\rm mm}(\bar{\beta},Z,N)=M_{\rm lq}^{\rm S}(Z,N)+E_{\rm corr}(\bar{\beta},Z,N)\tag{34}$$

and therefore

$$E_{\rm def}(\bar{\beta},Z,N)=E_{\rm corr}(\bar{\beta},Z,N)-E_{\rm shell}^{\rm S}(Z,N)-V_{\rm mm}^{\rm pair}(0,Z,N).\tag{35}$$

By inserting this expression for $E_{\rm def}(\bar{\beta},Z,N)$ in Eq. (33) we can express $\langle V_{\rm FDSM}\rangle$ in terms of the more commonly used microscopic correction energy, which is the energy usually plotted as potential-energy surfaces. We then get

$$\begin{aligned}\langle V_{\rm FDSM}\rangle&=E_{\rm shell}^{\rm S}(^{208}{\rm Pb})-E_{\rm shell}^{\rm S}(Z,N)+E_{\rm smo\text{-}FG}(^{208}{\rm Pb})\\&\quad-E_{\rm smo\text{-}FG}(Z,N)-V_{\rm sh}^{\rm pair}(Z,N)+E_{\rm corr}(\bar{\beta},Z,N)\\&\quad+\delta E_{\rm diff}(Z,N).\end{aligned}\tag{36}$$

This expression differs from the one in Eq. (33) in that the spherical shell correction $E_{\rm shell}^{\rm S}(Z,N)$ now appears explicitly instead of the spherical pairing energy $V_{\rm mm}^{\rm pair}(0,Z,N)$. The five first terms in Eq. (36) can be calculated independently of the FDSM since they depend only on the spherical single-particle energies and on the Fermi-gas model. The difference between the sum of $\langle V_{\rm FDSM}\rangle$ and these terms is $E_{\rm corr}(\bar{\beta},Z,N)+\delta E_{\rm diff}(Z,N)$. In the region where the FDSM parameters were adjusted to nuclear masses $\delta E_{\rm diff}(Z,N)$ is small. Thus what is in the FRDM the microscopic correction to the spherical liquid-drop energy, $E_{\rm corr}(\bar{\beta},Z,N)$, is in the FDSM given solely by the polynomial parameter fit of $\langle V_{\rm FDSM}\rangle$. Such a description can hardly be considered a solid microscopic foundation of a model.

E. A comparison between the FDSM versions I and II

Finally we shall make a brief comparison of version I and version II of the FDSM mass formula. In version I [2] the nuclear mass was given by

$$M_{\mathrm{I}} = M(^{208}\mathrm{Pb}) + n_{\mathrm{p}} M_{\mathrm{p}} + n_{\mathrm{n}} M_{\mathrm{n}} + \langle H_{\mathrm{FDSM}} \rangle . \tag{37}$$

In this equation $\langle H_{\mathrm{FDSM}} \rangle$ is the expectation value of the FDSM Hamiltonian. Its value is given relative to the mass of ^{208}Pb and it does not include the mass excess of the additional $n_{\mathrm{p}} = Z - 82$ protons and $n_{\mathrm{n}} = N - 126$ neutrons, which are therefore added explicitly together with the mass of ^{208}Pb in Eq. (37). The expectation value of the FDSM Hamiltonian, $\langle H_{\mathrm{FDSM}} \rangle$, must not be confused with the FDSM shell correction $\langle V_{\mathrm{FDSM}} \rangle$. According to the FDSM paper [1], $\langle H_{\mathrm{FDSM}} \rangle$ incorporates the spherical liquid-drop energy and the spherical s.p. (and presumably also pairing) corrections, which are not contained in $\langle V_{\mathrm{FDSM}} \rangle$.

We now introduce the difference between the masses predicted by versions I and II as

$$\delta E_{\mathrm{I\text{-}II}} = M_{\mathrm{I}} - M_{\mathrm{II}} \tag{38}$$

and subtract Eq. (37) from Eq. (2). This gives after rearrangement of the terms

$$\begin{aligned} \langle H_{\mathrm{FDSM}} \rangle - \langle V_{\mathrm{FDSM}} \rangle = {} & M^{\mathrm{S}}_{\mathrm{lq}}(Z,N) + M^{\mathrm{s.p.}}_{\mathrm{sh}}(Z,N) + V^{\mathrm{pair}}_{\mathrm{sh}}(Z,N) \\ & - M(^{208}\mathrm{Pb}) - n_{\mathrm{p}} M_{\mathrm{p}} - n_{\mathrm{n}} M_{\mathrm{n}} \\ & + \delta E_{\mathrm{I\text{-}II}}(Z,N) . \end{aligned} \tag{39}$$

This expression simply verifies the difference between $\langle H_{\mathrm{FDSM}} \rangle$ and $\langle V_{\mathrm{FDSM}} \rangle$ described above, provided that the spherical s.p. correction is defined as $M^{\mathrm{s.p.}}_{\mathrm{sh}}(Z,N)$.

By introducing the proper expressions for $M^{\mathrm{s.p.}}_{\mathrm{sh}}(Z,N)$ given by Eq. (25), $n_{\mathrm{p}} = Z - 82$, and $n_{\mathrm{n}} = N - 126$, we obtain for Eq. (39)

$$\begin{aligned} \langle H_{\mathrm{FDSM}} \rangle - \langle V_{\mathrm{FDSM}} \rangle = {} & E^{\mathrm{S}}_{\mathrm{shell}}(Z,N) + V^{\mathrm{pair}}_{\mathrm{sh}}(Z,N) + M^{\mathrm{S}}_{\mathrm{lq}}(Z,N) \\ & - E^{\mathrm{S}}_{\mathrm{shell}}(^{208}\mathrm{Pb}) - E_{\mathrm{smo\text{-}FG}}(^{208}\mathrm{Pb}) \\ & + E_{\mathrm{smo\text{-}FG}}(Z,N) - M(^{208}\mathrm{Pb}) \\ & - (Z-82) M_{\mathrm{p}} - (N-126) M_{\mathrm{n}} \\ & + \delta E_{\mathrm{I\text{-}II}}(Z,N) \end{aligned} \tag{40}$$

in which the true spherical Strutinsky shell-correction energy $E^{\mathrm{S}}_{\mathrm{shell}}(Z,N)$ appears explicitly together with the undesirable terms that are present in Eq. (25). It should be observed that these terms are introduced through $\langle V_{\mathrm{FDSM}} \rangle$ and not through $\langle H_{\mathrm{FDSM}} \rangle$, which therefore is physically more appealing. In spite of the undesirable terms, the expression for $\langle H_{\mathrm{FDSM}} \rangle - \langle V_{\mathrm{FDSM}} \rangle$ has some interesting properties. Since the predicted masses are similar to within about 1 MeV for the two models, at least for nuclei with known masses, we may for such nuclei neglect the term $\delta E_{\mathrm{I\text{-}II}}(Z,N)$. All the other terms are either constants or smooth functions of N and Z except $E^{\mathrm{S}}_{\mathrm{shell}}(Z,N)$ and $V^{\mathrm{pair}}_{\mathrm{sh}}(Z,N)$ but they are all independent of the FDSM itself. The energy resulting from these terms does therefore not depend on the fitted FDSM constants, nor on whether the SU(2) or SU(3) version of the FDSM is used.

Since both $\langle H_{\mathrm{FDSM}} \rangle$ and $\langle V_{\mathrm{FDSM}} \rangle$ are described by polynomial expressions, also the difference between the two terms is a polynomial expression, i.e., the left-hand side of Eq. (40) is a polynomial expression. This implies that only if the right-hand side of Eq. (40), with $\delta E_{\mathrm{I\text{-}II}}(Z,N) = 0$, can be written as a polynomial expression, can the two versions of the FDSM mass formula give the same masses. As it turns out, this is not possible. Only over a limited range in N and Z can it be approximated by a polynomial expression. As a consequence, $\delta E_{\mathrm{I\text{-}II}}(Z,N) = 0$ will grow rapidly outside the local region of parameter adjustment. That this actually is the case is shown in Sec. V A.

F. Octupole effects

In their first global mass calculation in 1981 [19] Möller and Nix showed that the large deviation obtained between calculated and measured masses in the vicinity of ^{222}Ra would disappear if the energy were minimized also with respect to octupole shape degrees of freedom. However, although the source of the deviations in the ^{222}Ra region were understood at the time, no global calculation with octupole deformations taken into account were carried out until 1992 [28]. In the 1981 calculation only symmetric P_2 and P_4, were considered whereas in 1992 both symmetric P_6 and mass-asymmetric P_3 distortions were taken into account in addition to the P_2 and P_4 deformations considered in 1981. For ^{222}Ra it was found that the inclusion of P_6 deformations lowered the energy by about 0.7 MeV and that the subsequent inclusion of P_3 deformations lowered the ground-state energy by an additional 1 MeV.

The results of the above study suggests that if octupole shape degrees of freedom *are not* taken into account in a mass calculation, then one would expect in the region around ^{222}Ra correlated errors in the calculated masses of up to about 1 MeV. One may of course argue that the results obtained in 1992 [28] and earlier by use of the macroscopic-microscopic method are incorrect and that there are no octupole effect on the nuclear masses. However, Leander and co-workers have in their series of papers [29–31] shown that there is a large body of nuclear-structure features of nuclei in the vicinity of ^{222}Ra that are most convincingly and consistently explained only through the mechanism of a sizable, permanent octupole deformation in the ground state.

In addition, similar octupole effects on nuclear masses were observed both in Woods-Saxon [30] calculations and in a calculation with an extended Thomas-Fermi model with a Skyrme interaction (ETFSI-1) [32]. Although the Woods-Saxon calculations are also based on the macroscopic-microscopic model they are based on a single-particle potential that has been developed quite independently from the folded-Yukawa model. The ETFSI-1 model which is quite different from the FRDM and Woods-Saxon models, has been independently developed and employs a different effective force. The observation of an octupole effect of a magnitude of 1 MeV on nuclear masses also in this model shows that this effect occurs quite generally in nuclear-structure models that have been developed over the years and tested successfully in comparisons to a large number of low-energy nuclear properties.

In the FDSM mass calculation there is no octupole interaction. One would therefore expect that the calculated

masses would exhibit large, correlated deviations in the vicinity of ^{222}Ra, deviations that would only be removed if an octupole interaction were specifically included in the calculations. The absence of any characteristic deviation between the calculated FDSM masses and measured masses in this region is a clear indication that the model is overparameterized, so that it is able to fit any reasonable data set. Consequently, we are again led to the conclusion that the results of the FDSM model calculations are fortuitous and without any particular significance.

V. PARAMETER DETERMINATIONS AND EXTRAPOLATABILITY

We illustrate by a few examples how details of model parameter determination procedures strongly influence model properties. In particular we show that adjustments to data sets that are too small or limited for the type of model investigated will lead to an unphysical set of constants and a model that diverges when applied outside the region where the parameters were adjusted.

A. Extrapolation of the two versions of the FDSM

It may be quite meaningless to compare different mass formulas in regions where there are no known masses, since it is impossible to determine which model provides the better extrapolation. We clearly see from Fig. 5 that the FDSM and the FRDM predict quite different masses as we go away from nuclei with known masses. The authors of the FDSM paper claim that their extrapolations should be superior. It may therefore be of particular interest to compare the predictions of the two versions of the FDSM mass formula for nuclei with unknown masses. If the predictions of the two versions diverge, the authors of the FDSM paper obviously have a problem in extrapolating their models. If so, which version gives the better extrapolation? And they do diverge, as illustrated in Figs. 6, 7, and 8. Only a few nucleons away from the fitted masses differences of several MeV appear.

B. Inadequacy of limited adjustments

To demonstrate that it is fairly trivial to obtain an rms deviation of about 0.2 MeV between calculated and measured masses when the study is restricted to a single region between magic numbers we perform the following exercise. We adjust nine macroscopic model parameters to obtain the best fit between calculated and measured masses. However, instead of using 1654 measured masses between oxygen and the heaviest masses as we normally do, we consider only 246 known masses in the region $Z \geqslant 82$ and $N \geqslant 126$. This is fewer than the 332 masses considered in the FDSM work, because we do not include as data the masses given by Wapstra systematics as discussed above. We use the finite-range liquid drop mass model, a folded-Yukawa single particle potential and a Lipkin-Nogami pairing interaction. This model represents a newer version of the model [7] quoted in the FDSM work. In Fig. 9 we show the resulting deviations between calculated masses and measured masses for nuclei between oxygen and the heaviest elements. We first observe

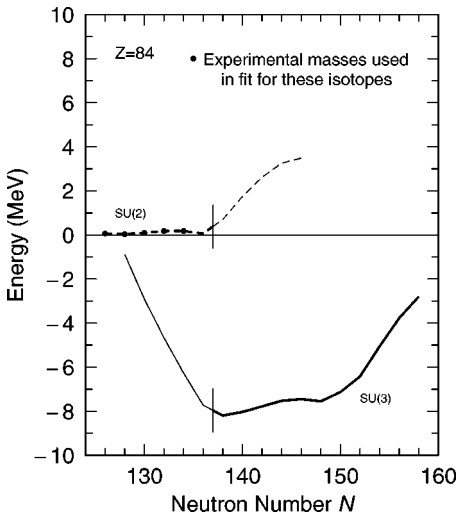

FIG. 6. Difference between calculated masses for the even-even Po isotopes in version I and version II of the FDSM. Both versions have been fitted to experimental masses for the neutron numbers indicated by black dots. For these neutron numbers the difference between the two versions is very small. The vertical solid lines indicate where the symmetry is assumed to change from SU(2) to SU(3) in version II. The solid curve shows the difference between version II masses and masses calculated with the SU(3) constants of version I and the masses of version II. The dashed curve shows the difference between masses calculated with the SU(2) constants of version I and the masses of version II. The curves have been extended a few neutron numbers beyond the symmetry transition point of version II.

that in the region of adjustment we obtain, with only nine parameters readjusted to this particular region an error that is very close to the error 0.22 MeV obtained in the FDSM work. In addition we clearly observe that the model strongly diverges outside the region where its parameters were adjusted. From this observation and from other studies one may conclude that to be physically interesting and significant a mass model should be formulated so that several spherical and deformed regions are described with a single set of constants.

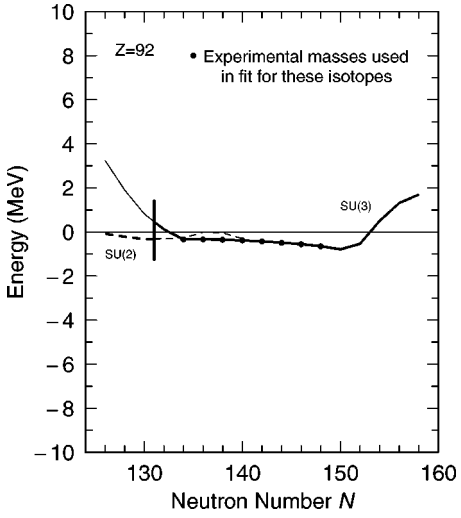

FIG. 7. Same as Fig. 6, but for the U isotopes.

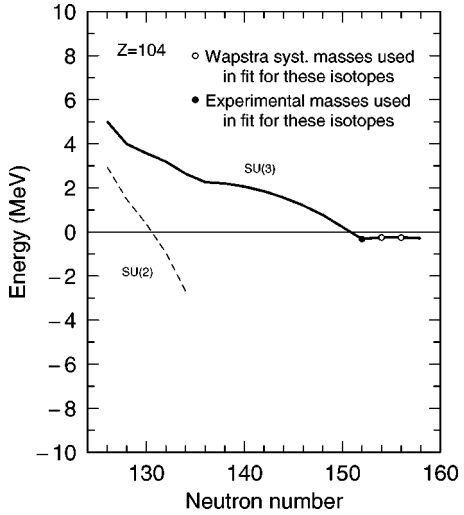

FIG. 8. Same as Fig. 6, but for the Rf isotopes. In this case only one experimental mass was available, when the FDSM parameters were fitted, but two masses extrapolated by Wapstra were also used.

C. Extrapolatability of mass models

We have shown above that macroscopic-microscopic models with constants that were determined by adjustments to too limited regions of nuclei are strongly divergent when applied to studies outside the region where its constants were determined. Is there any reason to believe that models with constants that were determined from more extended regions of nuclei are less divergent or not divergent at all? Yes, there are several convincing studies that show that this is the case.

The original Möller-Nix mass model results published in 1981 [20] have been compared to 354 masses that were not known when the model results were published. For these new nuclei the error is just 10% larger than in the original region. A more modern version of the model [5] exhibits only a 2% increase in the same case, which was now simulated by limiting the model adjustment to the old 1981 data set.

An investigation of the extrapolatability towards the heavy region has also been carried out. In this case the model parameters were adjusted only to nuclei with $A \leqslant 208$. The error for this region plus all heavier known nuclei (that were not included in this adjustment) was about 0.745 MeV, compared to 0.669 MeV when all nuclei were included in the fit [5]. Also, very significantly, it was found that the masses obtained for nuclei in or close to the superheavy region did not depend critically on the data region used in the adjustment procedure. As representative example we choose $^{272}110$ in the center of the deformed super-heavy region of relatively neutron-deficient nuclei and $^{288}110$ which is obtained as the center of the spherical superheavy island in the FRDM (1992). For these two nuclei we obtained mass excesses of 133.82 and 165.68 MeV in the calculation based on adjusting the parameters to all nuclei from oxygen to the heaviest elements. In the limited adjustment to nuclei with $A \leqslant 208$ we obtained mass excesses of 133.65 and 166.79 MeV, respectively, for these two nuclei. In the more limited adjustment the heaviest nucleus was 80 nucleons away from the heaviest nucleus included in the adjustment.

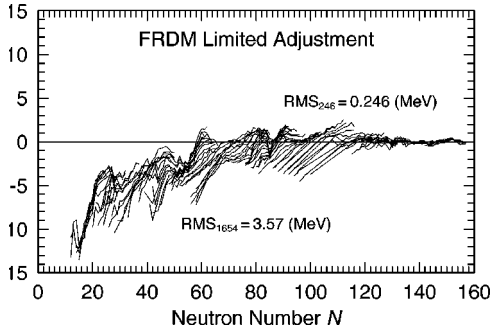

FIG. 9. Calculated model error for the case when macroscopic model parameters were adjusted only to the 246 available masses for nuclei with $Z \geqslant 82$ and $N \geqslant 126$.

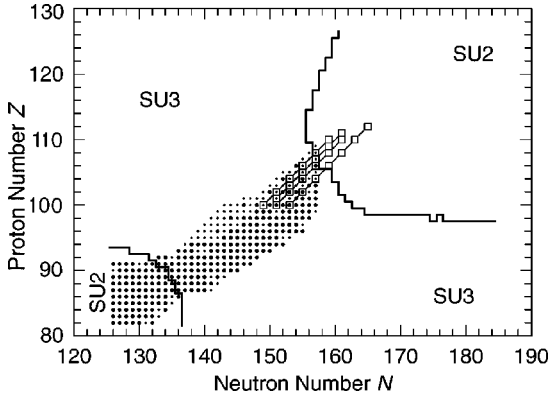

FIG. 10. Nuclear chart in the region where the FDSM mass formula is applicable. Large dots represent those masses for which measured values are given in the Audi 1989 mass evaluation [24]. Small dots represent nuclei for which Wapstra systematics was given in that evaluation. Squares show recently discovered α-decay chains. Regions with FDSM SU(2) and SU(3) symmetry are also shown.

VI. TESTING THE FRDM AND FDSM WITH NEW DATA

Some time after the parameters of the FRDM and FDSM were determined new experimental data became available at significant distances from previously known data, as shown in Figs. 10 and 11.

The data consist of four α decay sequences originating in $^{269}110$, $^{271}110$, $^{272}111$, and $^{277}112$, which were observed at GSI [33–35]. All these decay chains terminate in previously known α decays, which makes the identification of new nuclei unambiguous. These decay chains contain 17 different alpha decays for which the mother and daughter masses were not both known in 1992 when the FRDM and FDSM were adjusted.

The experimental Q_α values are compared to the theoretical predictions of the FDSM and FRDM models in Fig. 11. It should be observed that there are some ambiguities in this comparison. It is not proven that the experimentally observed decays correspond to ground-state to ground-state transitions. In particular in odd and odd-odd nuclei it is not unlikely that the transition goes from the ground state to an

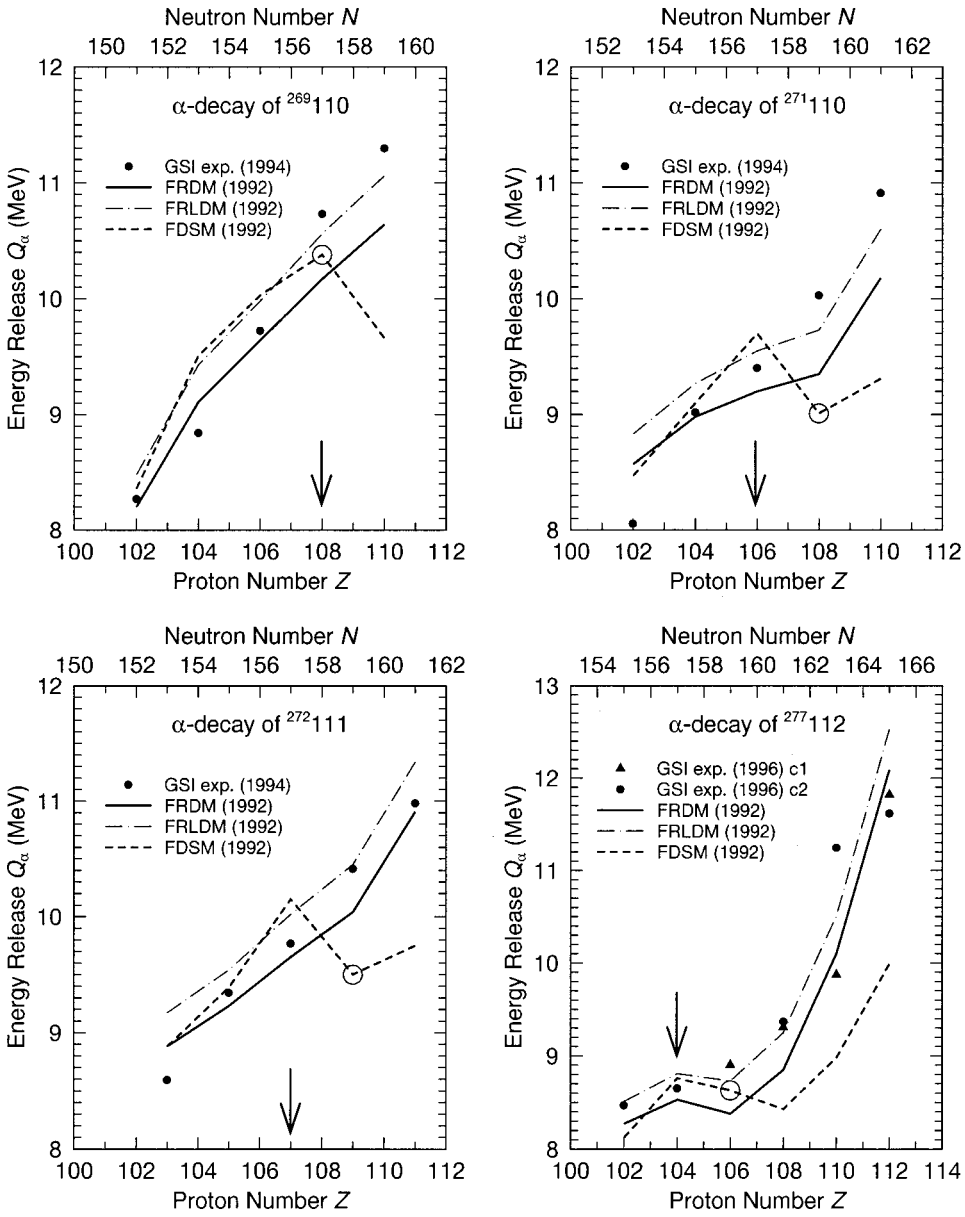

FIG. 11. Comparison between measured and calculated energy releases in α decay of four heavy nuclei. The experimental data are taken from Refs. [33,34], and [40]. The arrows indicate the heaviest nucleus included in the FDSM parameter fit. Circles show the transitions which involve an SU(2) mother nucleus and an SU3 daughter nucleus.

excited state due to selection rules [36,37]. It is less likely that a transition starts from an excited state, since the α lifetimes are long enough to allow, at least in most cases, the mother nucleus to deexcite to the ground state before emitting an α particle.

For the above reasons it can be assumed that the experimental Q_α values in many cases may be slightly smaller than the ones for the ground-state–to–ground-state transition, which is the theoretically calculated quantity. In general, the experimental Q_α values vary by at most a couple of hundred keV between different event chains. We then plot only one set of experimental Q_α values, namely the highest observed. In the case where large differences were observed between different decay chains namely for the decay starting at $^{277}112$ where the variation exceeds one MeV at $Z=110$ we plot both of the observed decay chains. Although the calculated Q_α values are obtained as ground-state–to–ground-state transitions but the experimental Q_α values may correspond to other transitions, the following can nevertheless be concluded: Within each experimental decay chain, Q_α increases without any exception with increasing mass (or proton) number. At proton number 102 Q_α has a value close to 8 MeV. At proton number 110, the value is close to 11 MeV.

For the decay chains starting at $Z=110$ and $Z=111$, the Q_α values of the FRDM show the same increasing trend as the experimental data. The slope, however, is smaller than in the data. In the decay chain starting at $Z=112$, the FRDM Q_α value decreases slightly from $Z=104$ to $Z=106$. The experimental values vary very little between $Z=102$ and $Z=106$, although they do increase. The overall agreement between the FRDM and experiment is very good for the chain starting at proton number 112. The rms error between the calculated FRDM Q_α values and the highest experimental Q_α values is 0.49 MeV for the 17 decays in Fig. 11 for

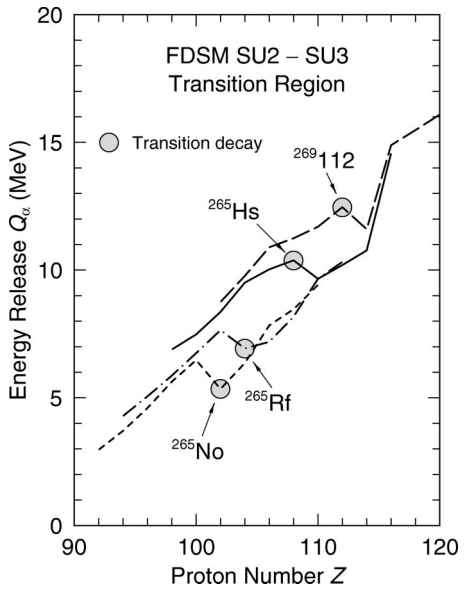

FIG. 12. α-decay chains in the FDSM model for $N-Z=45$, 49, 57, and 61. The figure illustrates the irregularities that occur when a decay chain passes from nuclei with SU(2) symmetry to nuclei with SU(3) symmetry. The transition point in each chain is indicated with a shaded circle.

which not both mother and daughter masses were known in 1992. Thus the FRDM extrapolates to this region without divergence since in the known region where the model parameters were fitted to known masses, the rms error for 1450 Q_α values is 0.65 MeV [38].

The Q_α values calculated with the FDSM show a very different behavior compared to those of the FRDM and the experimental data. In the lower end of each α-decay chain, the FDSM results agree with data about as well as the FRDM. This is for nuclei which were included in the fit of the FDSM parameters. However, immediately above the last fitted nucleus the Q_α values start to deviate strongly from the experimental data. In all four chains the FDSM Q_α curve bends down strongly one or two α decays beyond the last fitted nucleus. In the $Z=112$ decay chain, which extends higher above the last fitted nucleus than the three other chains, the FDSM chain resumes its increasing trend above the downbend but does not catch up with the experimental points.

In order to understand how Q_α can deviate so strongly from data immediately above the last fitted nucleus, it should be observed that the FDSM changes from SU(3) to SU(2) symmetry in close vicinity to the last fitted nucleus in the four new decay chains, see Figs. 10 and 11. The Q_α value corresponding to the decay from the last SU(2) nucleus in a chain to the first SU(3) nucleus is indicated with a circle in Fig. 11, whereas the heaviest nucleus included in the FDSM parameter fit is shown by an arrow. A comparison with Fig. 12 shows that it indeed is the transition between the SU(2) and SU(3) regions that causes the downbend and not the fact that we are passing beyond the region of fitted masses. Figure 12 shows four extended α chains, corresponding to $N-Z=61$ (transition point ^{265}No), $N-Z=57$ (transition point ^{265}Rf), $N-Z=49$ (transition point ^{265}Hs), and $N-Z=45$ (transition point ^{269}112). In all cases the obvious irregularity in the middle of the curves coincides with the transition between the SU(2) and SU(3) regions as can be seen from Fig. 10. The fact that the transition between the two symmetries appears at this location is a result of the Fermi blocking of the FDSM, which apparently can be associated with a clear downbend in the Q_α curves. The experimental Q_α values in Fig. 11 show no sign of a downbend, thus giving no support for a Fermi blocking in operation.

In Fig. 11 we have included also the results of the FRLDM model. It differs from the FRDM in using for the macroscopic energy the finite-range liquid-drop model instead of the finite-range droplet model. The FRLDM had a model error of 0.779 MeV in the fitted region, in contrast to the FRDM for which the model error is 0.669 MeV [5]. However, the FRLDM has two fewer adjustable parameters than does the FRDM.

Although the FRLDM has a higher model error taken over all known masses than does the FRDM, it seems to agree better with data for the high Z α-decay chains, perhaps because models with fewer parameters often extrapolate better. However, it is not for this purpose it is included in Fig. 11. It is rather for illustrating that although the top end of the chains lies about eight or more nucleons away from the last fitted one, the two versions of the macroscopic-microscopic model both extrapolate very well, giving Q_α values which differ only by a few hundred keV. This should be compared with the two versions of the FDSM, for which the calculated masses differ by several MeV, just a few nucleons away from the last fitted nucleus as illustrated in Figs. 6–8.

The heaviest experimental mass, used in the fit of the FRDM and FRLDM constants, is that of ^{263}Sg. The heaviest nucleus in the GSI chains is ^{277}112, which thus is eight neutrons and six protons away from the heaviest nucleus included in the parameter fit. It is evident from Fig. 11 that the FRDM and FRLDM masses, and hence the Q_α values, can be extrapolated over such distances without deviating much from each other. On the other hand, the extrapolation of the FDSM gives masses and Q_α values, which deviate significantly from the other two models and from the experimental data. It therefore becomes evident that the FDSM fails completely to describe the new experimental data in the heavy SU(2) region whereas the FRDM achieves similar accuracy here as in the region of known nuclei where its parameters were determined.

VII. CONCLUSIONS

Counting the number of model constants and trying to relate it to the quality of a model and to how well a model can be extrapolated to unknown regions is not a straightforward task. Parameters are of many different kinds, but all must be given numerical values in order to calculate a value for an observable quantity, e.g., the mass of a nucleus. Some constants have since long well-established values and may not even be thought of as parameters. On the other end of the scale are completely ''free'' parameters, whose values are determined by a least-squares fit to some of the experimental

quantities a model is supposed to describe. In the FRDM all of these free parameters and the values obtained have a straightforward physical interpretation.

Since the number of model parameters has been made one of the main issues by the proponents of the FDSM model, we have in this paper described the model at a level of detail that allows every single model parameter to be identified and we have made a consistent count of the number of parameters in the model. In our opinion it is clear that the claim in Ref. [1] that *''Thus we have reduced the number of adjustable parameters in the FDSM-Strutinsky mass formula from 16 in version I to 13 in version II''* is a gross misrepresentation of the number of adjustable parameters in the FDSM, by any criteria for labelling a parameter ''adjustable.'' However, considering also what is said in the previous paragraph, we leave it open to the reader to draw further conclusions. Instead, we shall concentrate on the conclusions that can be drawn from the experimental data which recently have become available.

The new experimental data on Q_α values, and thus differences between nuclear masses, in the superheavy region show that the mass formula derived from the FDSM cannot be extrapolated to describe those masses. Several reasons for this failure could be identified.

(1) The specific formulation of the model, used for deriving the mass formula, is restricted to nuclei in the region with proton numbers between $Z=82$ and $Z=126$ and neutron numbers between $N=126$ and $N=184$. To fit the free model parameters only experimental masses of nuclei in this region can be used. There were, when the parameters were fitted, only 246 experimental masses available. The distance from the heaviest nucleus for which an experimental mass was available ($Z=106$, $N=157$) to the center of the historical superheavy region at $Z=114$ and $N=184$ is 8 units in proton number and 27 units in neutron number and to the doubly magic nucleus $Z=126$ and $N=184$ (the heaviest nucleus covered by the FDSM mass formula) is 20 units in proton number and 27 units in neutron number. The extrapolation needed to reach these nuclei is therefore very long, considering that the experimental masses used in the fit only covers 24 units in proton number and 31 units in neutron number. The FDSM mass predictions for the heaviest nuclei can therefore be expected to be very uncertain.

(2) In addition to the experimental masses another 86 masses, estimated (extrapolated) according to Wapstra systematics [24], were used in the fit of the FDSM parameters. The reliability of these masses is hard to judge, but experience shows that the error is considerably larger than the error claimed for the FDSM masses. Including these ''Wapstra systematics'' masses in the parameter fit implies that uncontrollable errors are built into the FDSM mass formula. Since the Wapstra systematics masses typically lie at the border of the region of the experimentally known masses, they will have a particularly bad influence on how the FDSM mass formula extrapolates to unknown mass regions.

(3) The FDSM parameters are divided into two sets. One for nuclei with SU(2) symmetry, including nuclei in the vicinity of the doubly magic nucleus ^{208}Pb as well as a large number of nuclei in the superheavy region below the doubly magic nucleus at $Z=126$ and $N=184$. Experimental masses for SU(2) nuclei were only available in the region around ^{208}Pb when the FDSM masses were fitted. In the superheavy region only two Wapstra systematics masses were available. Except for the guidance given by these two masses, the FDSM masses in the superheavy SU(2) region are the result of a long-range extrapolation from the SU(2) region near ^{208}Pb. The FDSM masses in the superheavy SU(2) region can therefore be expected to have particularly large errors, which has now been confirmed by the recently available Q_α values in this region.

The second parameter set should be used for nuclei with SU(3) symmetry, located in between the two regions with SU(2) symmetry. SU(3) nuclei with known masses lie in a compact region. Only eight new masses with SU(3) symmetry have become available since the parameters were fitted. Because they are just next to the region of previously known masses it is not possible to evaluate the quality of the SU(3) constants and the extrapolative reliability of the FDSM by comparing with this limited data set.

(4) The $\langle V_{\mathrm{FDSM}} \rangle$ term in the FDSM mass formula contains a complete second-order expression in N_p and N_n with adjustable coefficients in front of each term, which should be an appropriate expression in the symmetry limits. However, when inserted in the mass formula and used for fitting nuclear masses, the second-order expression does not only contain the proper FDSM energy but must also compensate for the difference between the smooth Strutinsky energy and the Fermi-gas energy. This energy difference can only locally be described with high accuracy using a second-order expansion in N_p and N_n. The ranges between the magic proton numbers 82 and 126 and the magic neutron numbers 126 and 184 are too long to qualify as local. On the other hand, the region covered by experimental data, can be considered as local, at least when divided into one SU(2) and one SU(3) region with a separate parameter set for each region. This explains why the FDSM mass formula reproduces the experimental masses with high accuracy (although no higher than a locally adjusted FRDM), but also why it cannot, not even in principle, be used for long-range extrapolations, which are needed to, e.g., predict masses in the historical superheavy region.

We have shown that the FRDM mass model agrees much better with the new experimental data than does the FDSM mass formula. The reason for this is best understood by noting four corresponding criteria which governed the development of the FRDM:

(1) The FRDM mass model was fitted to all experimental masses from $Z=N=8$ to $Z=106$, $N=157$ known at the time of the fit. In total 1654 experimental masses were available. Predicting masses in the superheavy region requires an extrapolation over the same number of additional protons and neutrons as in the FDSM case. However, a very long range of proton numbers (in total 99) and neutron numbers (in total 150) were included in the fit. Extrapolation to the superheavy region, 20 to 30 protons and neutrons above the heaviest nucleus considered in the fit, can therefore be made with some degree of confidence, which has now been confirmed by the new data.

(2) Only experimentally measured masses were included in the fit.

(3) A single set of constants were used for all nuclei.

(4) All terms in the FRDM mass model have a physically derived and well justified functional dependence on the proton and neutron numbers. This prevents rapid uncontrollable divergences outside the region covered by the fit.

ACKNOWLEDGMENT

This work was supported by the U. S. Department of Energy.

[1] X.-L. Han, C.-L. Wu, D. H. Feng, and M. W. Guidry, Phys. Rev. C **45**, 1127 (1992).
[2] C.-L. Wu, X.-L. Han, M. W. Guidry, and D. H. Feng, Phys. Lett. B **194**, 447 (1987).
[3] P. Möller, W. D. Myers, W. J. Swiatecki, and J. Treiner, *Proceedings of the 7th International Conference on Nuclear Masses and Fundamental Constants, Darmstadt-Seeheim*, 1984 (Lehrdruckerei, Darmstadt, 1984), p. 457.
[4] P. Möller, W. D. Myers, W. J. Swiatecki, and J. Treiner, At. Data Nucl. Data Tables **39**, 225 (1988).
[5] P. Möller, J. R. Nix, W. D. Myers, and W. J. Swiatecki, At. Data Nucl. Data Tables **59**, 185 (1995).
[6] C.-L. Wu, M. W. Guidry, and D. H. Feng, Phys. Lett. B **387**, 449 (1996).
[7] P. Möller and J. R. Nix, At. Data Nucl. Data Tables **39**, 213 (1988).
[8] V. M. Strutinsky, Nucl. Phys. **A95**, 420 (1967).
[9] V. M. Strutinsky, Nucl. Phys. **A122**, 1 (1968).
[10] S. G. Nilsson, K. Dan. Vidensk. Selsk. Mat. Fys. Medd. **29**, No. 16 (1955).
[11] D. Bés and Z. Szymański, Nucl. Phys. **28**, 42 (1961).
[12] Z. Szymański, Nucl. Phys. **28**, 421 (1961).
[13] A. Sobiczewski, Nucl. Phys. **A93**, 501 (1967).
[14] W. D. Myers and W. J. Swiatecki, Nucl. Phys. **81**, 1 (1966).
[15] L. Spanier and S. A. E. Johansson, At. Data Nucl. Data Tables **39**, 259 (1988).
[16] W. D. Myers, Nucl. Phys. **A145**, 387 (1970).
[17] D. G. Madland and J. R. Nix, Bull. Am. Phys. Soc. **31**, 799 (1986).
[18] D. G. Madland and J. R. Nix, Nucl. Phys. **A476**, 1 (1988).
[19] P Möller and J. R. Nix, Nucl. Phys. **A361**, 117 (1981).
[20] P. Möller and J. R. Nix, At. Data Nucl. Data Tables **26**, 165 (1981).
[21] W. D. Myers and W. J. Swiatecki, Ann. Phys. (N.Y.) **55**, 395 (1969).
[22] W. D. Myers, *Droplet Model of Atomic Nuclei* (IFI/Plenum, New York, 1977).
[23] P. Möller, J. R. Nix, and W. J. Swiatecki, Proceedings of the Winter Workshop on Nuclear Dynamics V, Sun Valley, Idaho, 1988, Michigan State University report, 1989, p. 5.
[24] G. Audi, Midstream Atomic Mass evaluation, private communication, 1989, with four revisions.
[25] A. H. Wapstra, G. Audi, and R. Hoekstra, At. Data Nucl. Data Tables **39**, 281 (1988).
[26] A. H. Wapstra and K. Bos, At. Data Nucl. Data Tables **19**, 175 (1977).
[27] A. H. Wapstra and K. Bos, At. Data Nucl. Data Tables **20**, 126 (1977).
[28] P. Möller, J. R. Nix, W. D. Myers, and W. J. Swiatecki, Nucl. Phys. **A536**, 61 (1992).
[29] G. A. Leander, R. K. Sheline, P. Möller, P. Olanders, I. Ragnarsson, and A. J. Sierk, Nucl. Phys. **A388**, 452 (1982).
[30] W. Nazarewicz, P. Olanders, I. Ragnarsson, J. Dudek, G. A. Leander, P. Möller, and E. Ruchowska, Nucl. Phys. **A429**, 269 (1984).
[31] G. A. Leander and Y. S. Chen, Phys. Rev. C **37**, 2744 (1988).
[32] Y. Aboussir, J. M. Pearson, A. K. Dutta, and F. Tondeur, Nucl. Phys. **A549**, 155 (1992).
[33] S. Hofmann, N. Ninov, F. P. Heßberger, P. Armbruster, H. Folger, G. Münzenberg, H. J. Schött, A. G. Popeko, A. V. Yeremin, A. N. Andreyev, S. Saro, R. Janik, and M. Leino, Z. Phys. A **350**, 277 (1995).
[34] S. Hofmann, N. Ninov, F. P. Heßberger, P. Armbruster, H. Folger, G. Münzenberg, H. J. Schött, A. G. Popeko, A. V. Yeremin, A. N. Andreyev, S. Saro, R. Janik, and M. Leino, Z. Phys. A **350**, 281 (1995).
[35] S. Hofmann, N. Ninov, F. P. Heßberger, P. Armbruster, H. Folger, G. Münzenberg, H. J. Schött, A. G. Popeko, A. V. Yeremin, S. Saro, R. Janik, and M. Leino, Z. Phys. A **354**, 229 (1996).
[36] M. A. Preston, *Physics of the Nucleus* (Addison-Wesley, Reading, MA, 1962).
[37] S. Ćwiok, W. Nazarewicz, and P. H. Heenen, Phys. Rev. Lett. **83**, 1108 (1999).
[38] P. Möller, J. R. Nix, and K.-L. Kratz, At. Data Nucl. Data Tables **66**, 131 (1997).
[39] S. G. Nilsson, C. F. Tsang, A. Sobiczewski, Z. Szymański, S. Wycech, C. Gustafson, I.-L. Lamm, P. Möller, and B. Nilsson, Nucl. Phys. **A131**, 1 (1969).
[40] S. Hofmann, Proceedings of the XV Nuclear Physics Divisional Conference on Low Energy Nuclear Dynamics, St. Petersburg, Russia, 1995.